COLLÈGE DE FRANCE
1530

Chaire de Physique de la Matière Condensée

Des oxydes supraconducteurs aux atomes froids

- la matière à fortes corrélations quantiques -

Antoine Georges

Cycle 2009-2010
Cours 7 – 16 juin 2010

Cours 7: Transition métal-isolant de Mott (II): le point de vue de la théorie de champ moyen dynamique

Séminaire:

COLLÈGE DE FRANCE
1530

Andrew J. MILLIS
Columbia University

Illuminating the Strong Correlation Problem:
Optical conductivity of manganites, nickelates and cuprates.

OUTLINE

- 1. Limitations of Brinkman-Rice
- 2. Introduction to Dynamical Mean-Field Theory
- 3. The effective hybridization function - a quantum generalization of the `Weiss field' concept
- 4. Phase diagram: Metal-insulator transition, magnetic phases
- 5. Nature of the metallic phase
- 6. Fragility of the Fermi-liquid state: the quasiparticle coherence scale
- 7. Beyond Fermi liquid: transport, spectroscopies (transfers of spectral weight)
- 8. The Mott critical endpoint

Qualitative features of Brinkman-Rice theory: (lecture 6)

- Quasiparticle weight vanishes as transition is reached: $\mathbf{Z \sim U_c - U}$ (BC) or $\mathbf{Z \sim \delta}$ (FC)
- Drude weight **~ Z**
- Effective mass $\mathbf{m^*/m = 1/Z}$: *quasiparticles become heavy as insulator is reached*
- Insulator is incompressible: jump in chemical potential $\mathbf{\Delta\mu \sim (U-U_c)^{1/2}}$
- Local susceptibility diverges at the transition $\chi_{loc} \sim 1/Z$ → insulator has local moments (ln2 entropy)
- Optical gap of insulator and uniform susceptibility not so well-defined in this theory (sometimes identified to $\Delta\mu$ and χ_{loc} , respectively, but see below.

The simplest self-energy which makes all this possible:

$$\Sigma(\omega) = \Sigma(0) + \omega\left(1 - \frac{1}{Z}\right)$$

1) Σ(0) is in charge of making Luttinger happy by insuring a Large Fermi surface: $\mu[n] - \Sigma[\omega = 0; n] = \mu_{U=0}[n]$

2) All the action is in Z ! no k-dependence→ $\frac{m^*}{m} = 1 - \frac{\partial\Sigma}{\partial\omega} = \frac{1}{Z}$

3) This self-energy is both extremely simple and a bit crazy:

- Crazy high-frequency behavior
- Only quasiparticles are described and they have infinitely long lifetime (Σ'' = 0)
-Total spectral weight is Z → incoherent part not included
-Don't even think of checking Kramers-Kronig…

Limitations of Brinkman-Rice :

cf. lecture 6 - *quite clear from the experimental results on Titanates-*

- → Must describe lifetime of quasiparticles
  → transport, optics
- Excited states: beyond quasiparticles (Hubbard satellites)
- Transfers of spectral weight
- Superexchange provides a cutoff to the divergence of effective mass (clear from entropic arguments)

2. Introduction to the Dynamical Mean-Field Theory framework

Correlated electrons in large dimensions:
W.Metzner & D.Vollhardt, 1989 (then@Aachen)
Dynamical Mean-Field Theory:
AG & G.Kotliar, 1991 (then@Princeton & Rutgers)

DMFT:
An ``effective atom'' approach.

*Replace the full solid by an **effective atom** hybridized, in a **self-consistent manner**, to an **energy-dependent environment** (effective medium)*

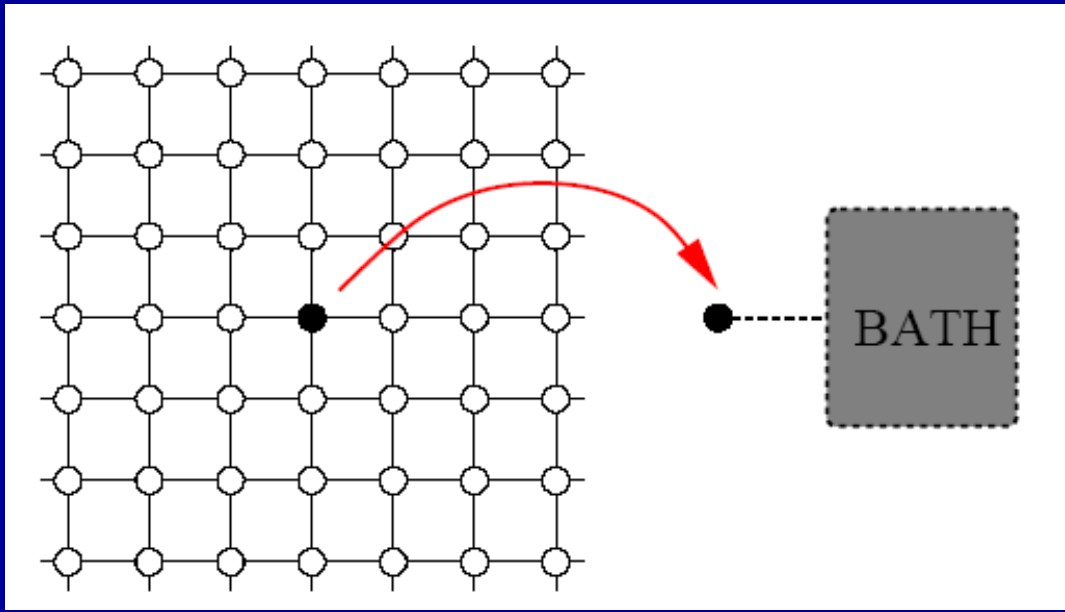

A simple example: the Hubbard model

$$H = -\sum_{\mathbf{R}\mathbf{R}'\sigma} t_{\mathbf{R}\mathbf{R}'} f^{\dagger}_{\mathbf{R}\sigma} f_{\mathbf{R}'\sigma} + \sum_{\mathbf{R}} H^{\mathbf{R}}_{\text{atom}}$$

Focus on a given lattice site:

Atom can be in 4 possible configurations: $|0\rangle, |\uparrow\rangle, |\downarrow\rangle, |\uparrow\downarrow\rangle$

Describe ``history'' of fluctuations between those configurations

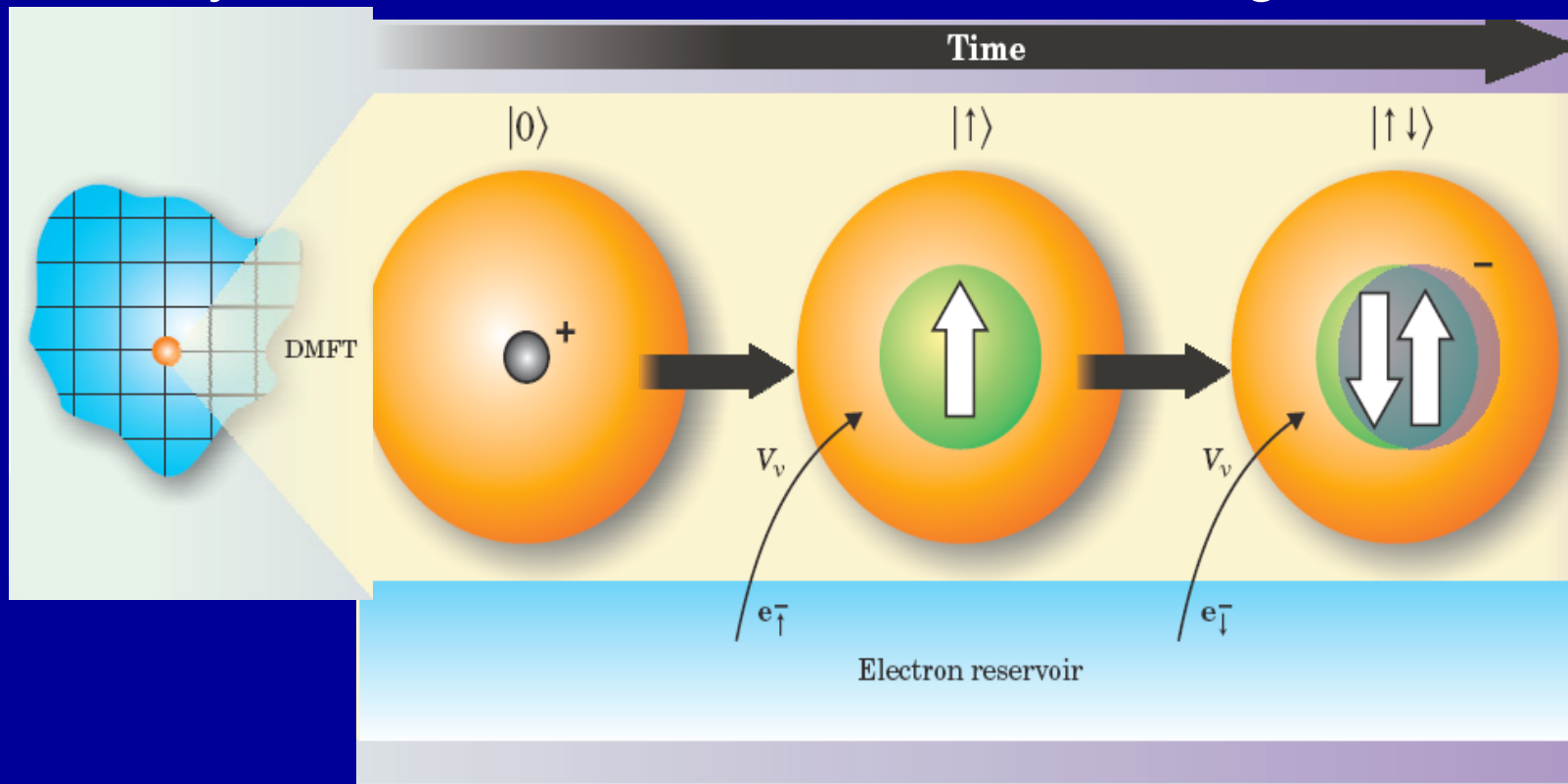

Atom is coupled to the environment by exchange of electrons: the dynamics of these histories is that of an Anderson impurity problem (cf. lectures 1-2)

As we have seen in lectures 1-2, an AIM is entirely specified by:

1) The position of the atomic level ε_d
2) The hybridization function $\Delta(\omega)$

$$
\begin{aligned}
S_{\text{eff}} &= \int_0^\beta d\tau \int_0^\beta d\tau' d_\sigma^\dagger(\tau)[(-\partial_\tau - \varepsilon_d)\delta(\tau-\tau') - \Delta(\tau-\tau')]d_\sigma(\tau') \\
&+ U\int_0^\beta d\tau n_\uparrow n_\downarrow
\end{aligned}
$$

At this stage, we have not yet specified how to choose ε_d and Δ

Focus on energy-dependent local observable :

$$G_{RR}(\omega) \equiv G_{\rm loc}$$

On-site Green's function (or spectral function) of the `solid'

Use atom-in-a-bath as a reference system to represent this observable:

→ IMPOSE that ε_d and Δ should be chosen such that:

$$G_{\rm imp}[\omega; \varepsilon_d, \Delta(\omega)] = G_{\rm loc}(\omega)$$

At this point, given G_{loc} of the lattice Hubbard model, we have just introduced an exact local representation of it

G_{RR} is related to the exact self-energy of the lattice (solid) by:

$$G_{\mathbf{RR}}(\omega) = \sum_{\mathbf{k}} \frac{1}{\omega + \mu - \varepsilon_{\mathbf{k}} - \Sigma(\mathbf{k}, \omega)} = G_{\mathsf{loc}}(\omega)$$

In which ε_k is the tight-binding band (FT of the hopping $t_{RR'}$)

High-frequency → $\varepsilon_d = -\mu + \sum_k \varepsilon_k \; (= -\mu)$

Let us now make the **APPROXIMATION** that the lattice self-energy is **k-independent** and coincides with that of the effective atom (impurity problem):

$$\Sigma(\mathbf{k}, \omega) \simeq \Sigma_{\mathsf{imp}}(\omega)$$

This leads to the following <u>self-consistency condition:</u>

$$G_{\mathsf{imp}}[i\omega; \Delta] = \sum_{\mathbf{k}} \frac{1}{G_{\mathsf{imp}}[i\omega; \Delta]^{-1} + \Delta(i\omega) - \varepsilon_{\mathbf{k}}}$$

DMFT equations: embedded atom + self-consistency

→ fully determines both the local G and Δ:

$$G_{\rm imp}[i\omega;\Delta] = \sum_{\mathbf{k}} \frac{1}{G_{\rm imp}[i\omega;\Delta]^{-1} + \Delta(i\omega) - \varepsilon_{\mathbf{k}}}$$

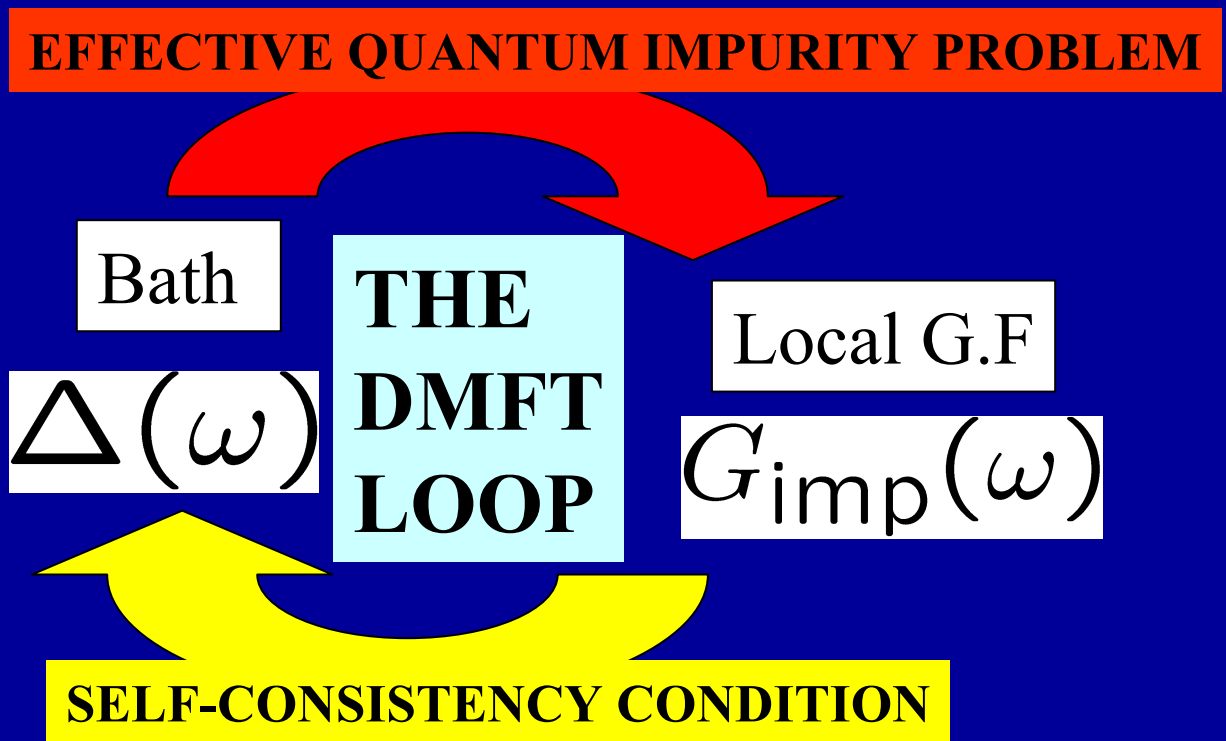

Weiss mean-field theory
Density-functional theory
Dynamical mean-field theory

} rely on similar conceptual basis

TABLE 2. Comparison of theories based on functionals of a local observable

Theory	MFT	DFT	DMFT
Quantity	Local magnetization m_i	Local density $n(x)$	Local GF $G_{ii}(\omega)$
Equivalent system	Spin in effective field	Electrons in effective potential	Quantum impurity model
Generalised Weiss field	Effective local field	Kohn-Sham potential	Effective hybridisation

- Exact energy functional of local observable

- Exact representation of local observable:
- Generalized ``Weiss field''
- Self-consistency condition, later approximated

see e.g:
A.G
arXiv cond-mat
0403123

Check two simple limits …

- Non-interacting case: $\Sigma=0$

$$G_{loc}^{U=0} = \mathcal{G}_0 = \sum_{\mathbf{k}} \frac{1}{i\omega_n + \mu - \epsilon_{\mathbf{k}}}$$

-"Atomic" limit (t=0):

4 states on each site: $|0\rangle, |\uparrow\rangle, |\downarrow\rangle, |\uparrow\downarrow\rangle$

Obviously, in this limit: $\Sigma_{ij}^{at} = \Sigma^{at}(i\omega_n)\,\delta_{ij}$

(Exact) atomic Green's function:

$$G_{at} = \frac{1 - n/2}{i\omega_n + \mu} + \frac{n/2}{i\omega_n + \mu - U}$$

$$\Delta(i\omega_n) = 0 \quad \mathcal{G}_0^{-1} = \frac{1}{i\omega_n + \mu}$$

The limit of large lattice connectivity

(Metzner&Vollhardt, 1989)

-The DMFT scheme becomes EXACT in the limit of large lattice connectivity (large number of spatial dimensions).

- Requires scaling of hopping amplitude $t_{ij} \propto 1/\sqrt{z}$

- Proof: e.g. ``cavity construction'' or perturbative inspection of Baym-Kadanoff functional.

Phases with long-range order

e.g self-consistency condition in commensurate Q=(π,…,π) antiferromagnetic phase

A- and B- sublattice, symmetry: $G_{A\sigma}(i\omega_n) = G_{B,-\sigma}(i\omega_n)$

Green's function matrix:

$$\begin{pmatrix} \zeta_{A\sigma} & -\epsilon_{\mathbf{k}} \\ -\epsilon_{\mathbf{k}} & \zeta_{B\sigma} \end{pmatrix}$$

$$\zeta_{A\sigma} = i\omega_n + \mu - \sigma h_s - \Sigma_{A\sigma}$$

Self-consistency:

$$G_{\alpha\sigma} = \zeta_{\bar{\alpha}\sigma} \int_{-\infty}^{\infty} d\epsilon \, \frac{D(\epsilon)}{\zeta_{A\sigma}\zeta_{B\sigma} - \epsilon^2}$$

Solving the effective quantum impurity problem: computational techniques

Several numerical algorithms, or semi-analytical approximation schemes have been developed over the years to this aim, starting in the early days of the Kondo effect (Anderson impurity model)

[e.g: Hirsch-Fye auxiliary field QMC,
Resummed perturbation theories,
Numerical Renormalisation Group]

Recent key advance:

continuous time QMC → cf seminar 1 by O.Parcollet

(A.Rubtsov et al.: pert. series in U,
P.Werner et al: pert. series around atomic limit)

Δ(ω): generalizing the Weiss field to the quantum world

Pierre Weiss
1865-1940
« Théorie du Champ Moléculaire »
(1907)

Einstein, Paul Ehrenfest, Paul Langevin, Heike Kammerlingh-Onnes, and Pierre Weiss at Ehrenfest's home, Leyden, the Netherlands. From Einstein, His Life and Times, *by Philipp Frank (New York: A.A. Knopf, 1947). Photo courtesy AIP Emilio Segrè Visual Archives.*

Low-frequency behavior of $\Delta(\omega)$ determines nature of the phase

- $\Delta(\omega \to 0)$ finite → local moment is screened. `Self-consistent' Kondo effect. Gapless metallic state.

- $\Delta(\omega)$ gapped → no Kondo effect, degenerate ground-state, insulator with local moments

A- Phase diagram

Will focus in the following (for lack of time) on:
-½ -filled Hubbard model
- mostly paramagnetic solutions

Generic phase diagram (Hubbard at ½-filling, schematic)

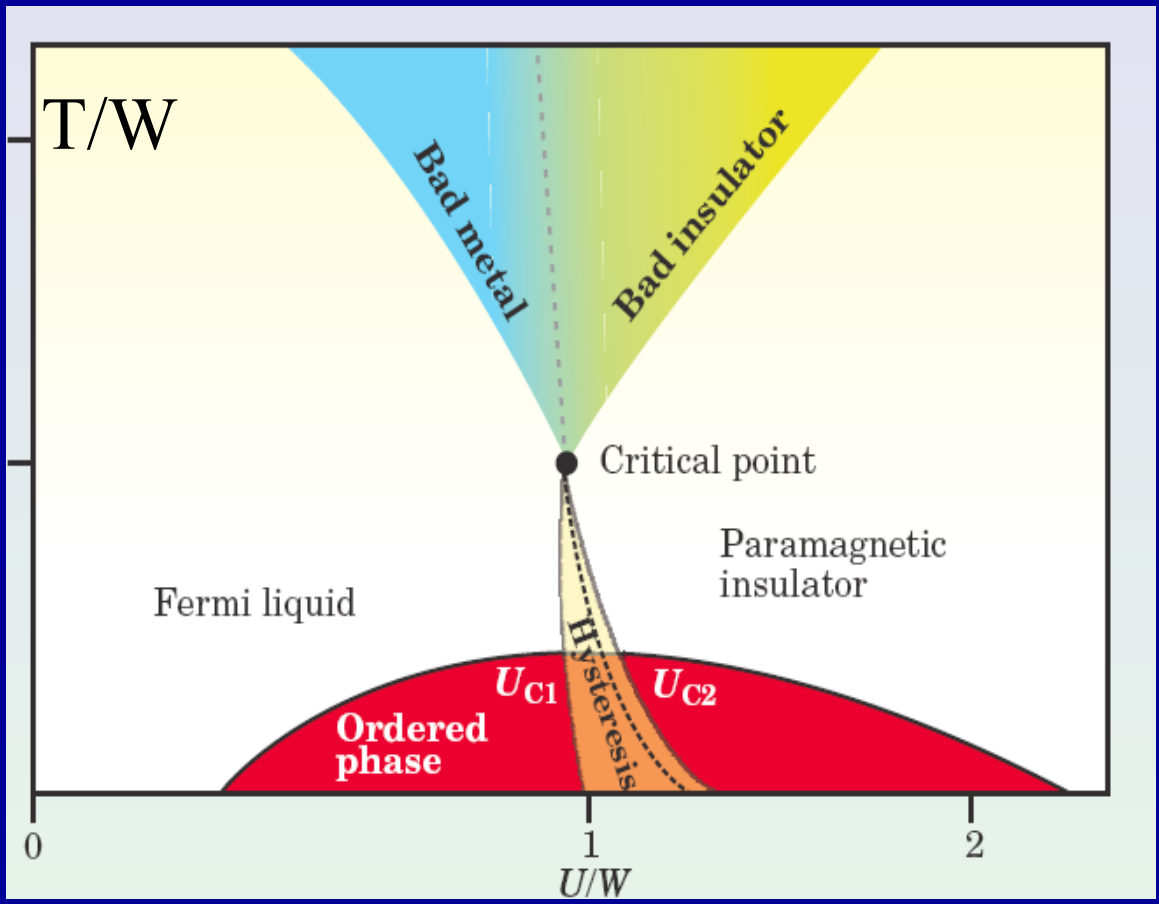

Unfrustrated ½-filled model: phases with long-range order and crossovers, d=3 cubic lattice

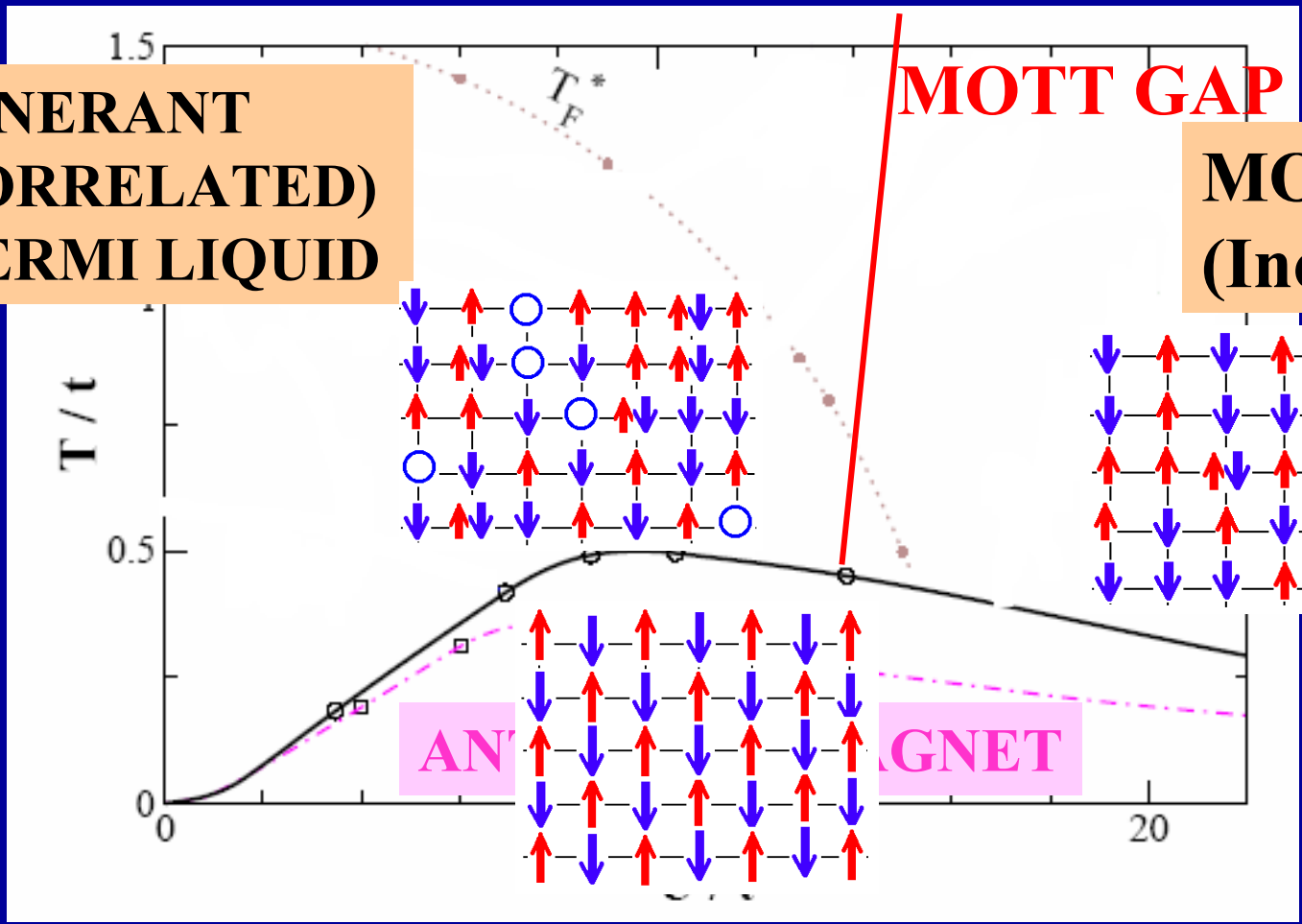

Critical boundary calculated for a 3D cubic lattice using:
-Quantum Monte Carlo (Staudt et al. Eur. Phys. J. B17 (2000) 411)
- Dynamical Mean-Field Theory approximation

Phase diagram : zoom on paramagnetic solutions

Hubbard model, Bethe lattice, homog. phase, $n = 1$, e.g., DMFT(QMC)

[Blümer '02]

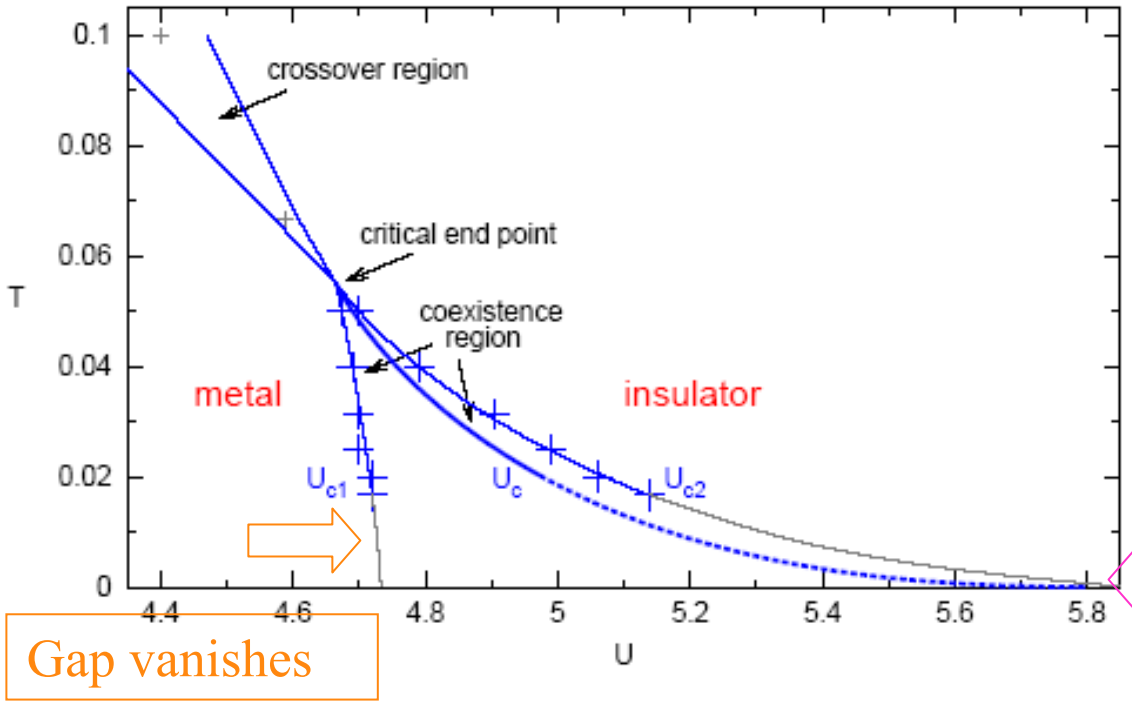

- coexistence region $[U_{c1}; U_{c2}]$, first-order transition
- crossover above critical region

Blümer et al. Units here are 4D=2*bandwidth

B-Nature of the metallic phase

- At (possibly very) low T,ω: a Fermi liquid

$$\mathrm{Re}\Sigma(\omega+i0^+)=U/2+(1-1/Z)\omega+O(\omega^3),$$
$$\mathrm{Im}\Sigma(\omega+i0^+)=-B\omega^2+O(\omega^4).$$

- At U_{c2} transition: Z→0 (~ Brinkman-Rice)
- Heavy quasiparticles:

m*/m=1/Z

(divergence reflects
large entropy of insulator,
see below)

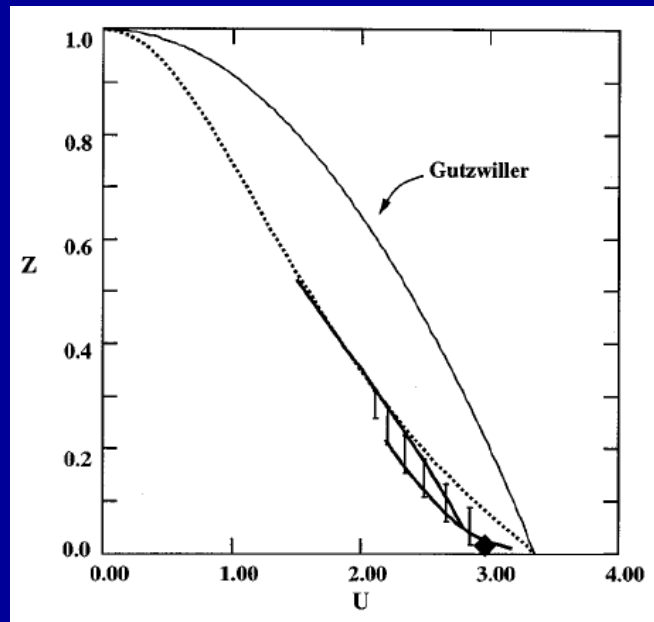

Approach to the Mott state in titanates

Saturation of m* in AF regime

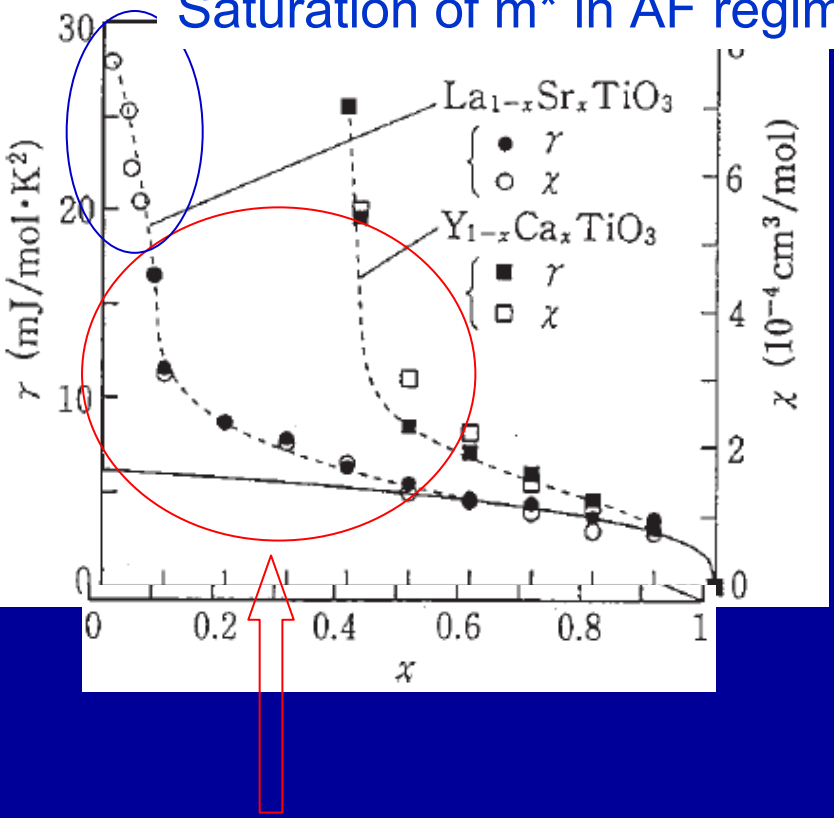

Increase of effective mass

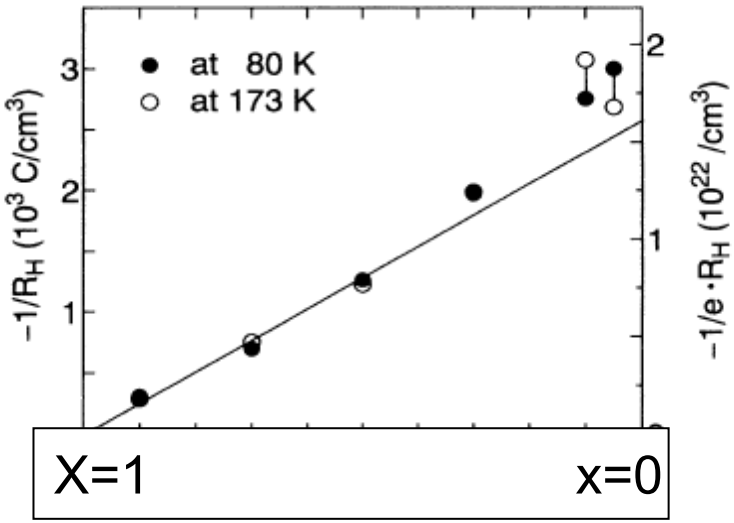

FIG. 2. The filling (x) dependence of the inverse of Hall coefficient (R_H^{-1}) in $Sr_{1-x}La_xTiO_3$. Open and closed circles represent the values measured at 80 K and 173 K, respectively. A solid line indicates the calculated one based on the assumption that each substitution of a Sr^{2+} site with La^{3+} supplies the compound with one electron-type carrier per Ti site.

R_H reported as ~ T-independent and consistent w/ large Fermi surface

Tokura et al.
PRL, 1993

But… there is (plenty of) life beyond the Fermi-liquid regime

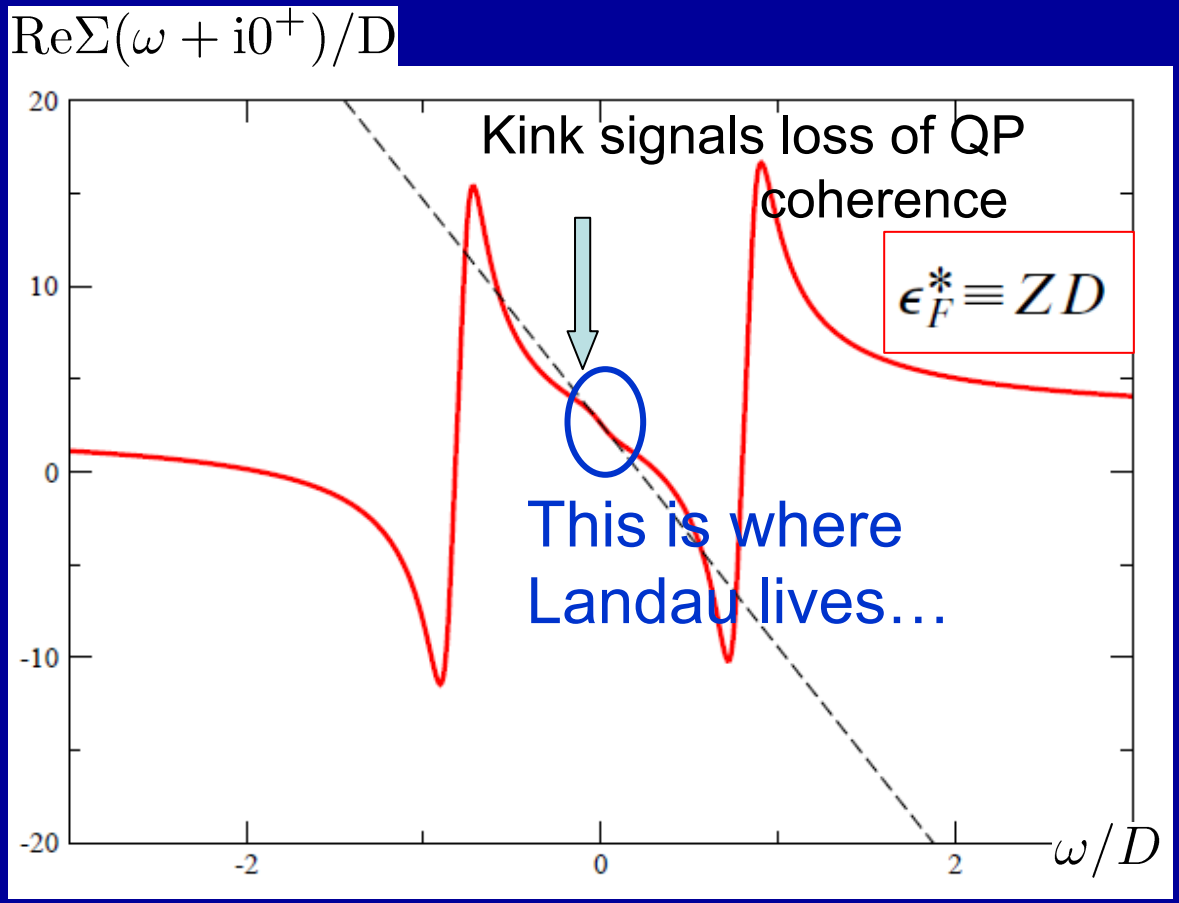

CTQMC+Analytical continuation (Pade),
courtesy M.Ferrero, compares perfectly to NRG

$B\omega^2$ applies only below coherence scale
B-coefficient is enhanced ~ $1/Z^2$

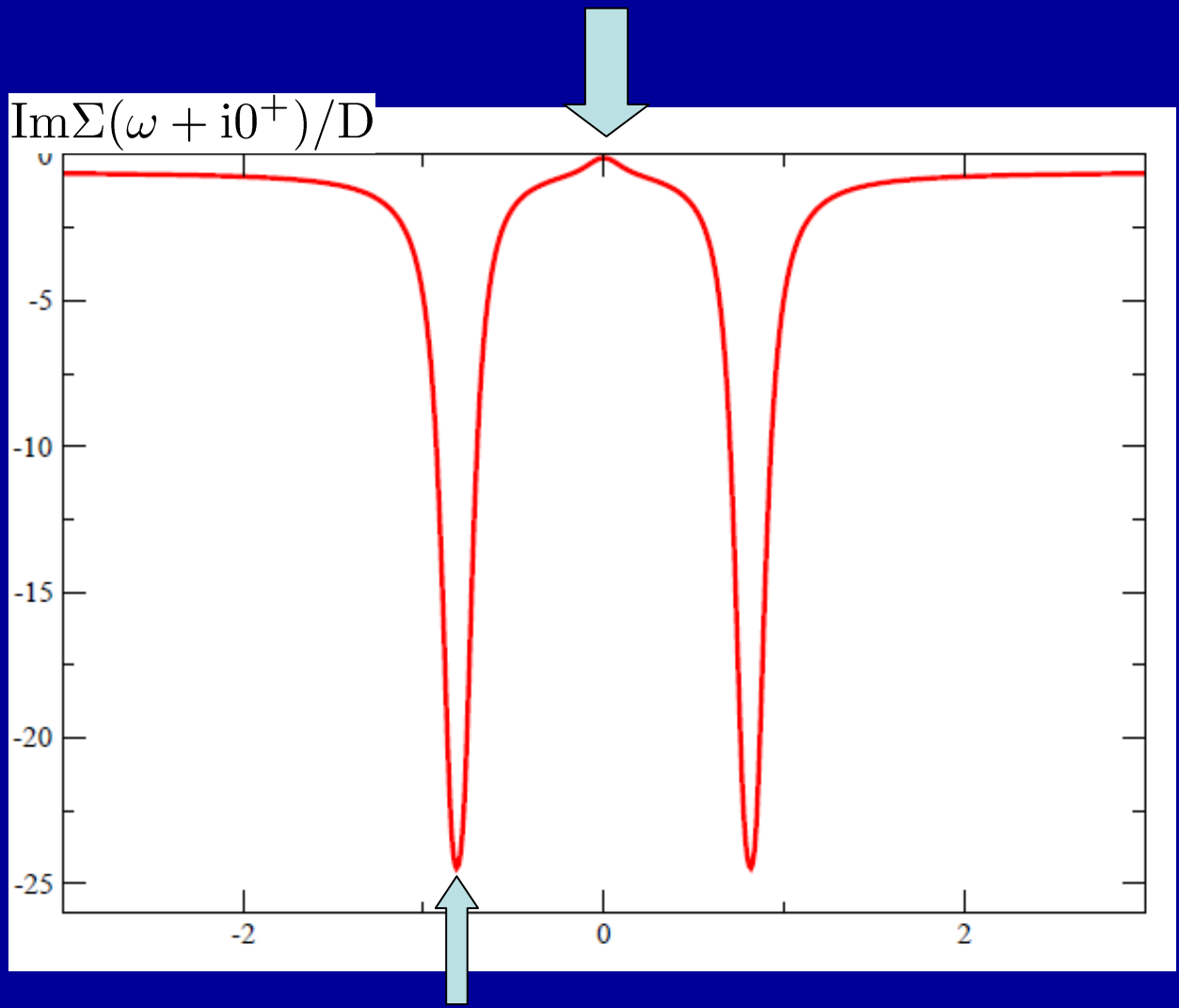

These 2 peaks will coalesce into a pole at $\omega=0$ as insulator is reached

k-integrated spectral function (total d.o.s) :

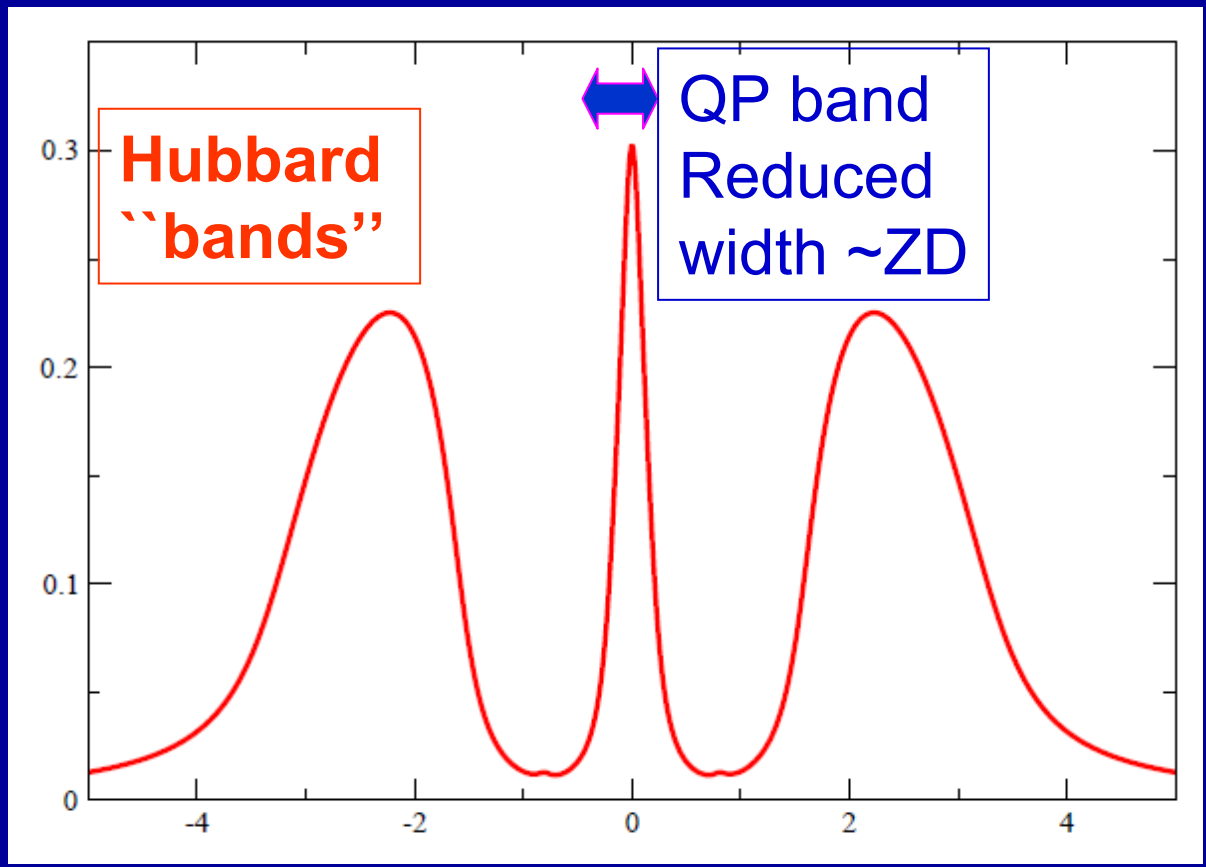

Value of A(ω=0) is pinned at U=0 value due to Luttinger theorem

→ Low-energy quasiparticles and incoherent Hubbard bands Coexist in one-particle spectrum of correlated metal

k-integrated spectral Function: early DMFT results

(AG&G.Kotliar 1992, AG&W.Krauth, M.Rozenberg et al. 1992-94)

Increasing U

Quasiparticle peak

$\Leftrightarrow$ QP bandwidth $\mathcal{E}_F^*$

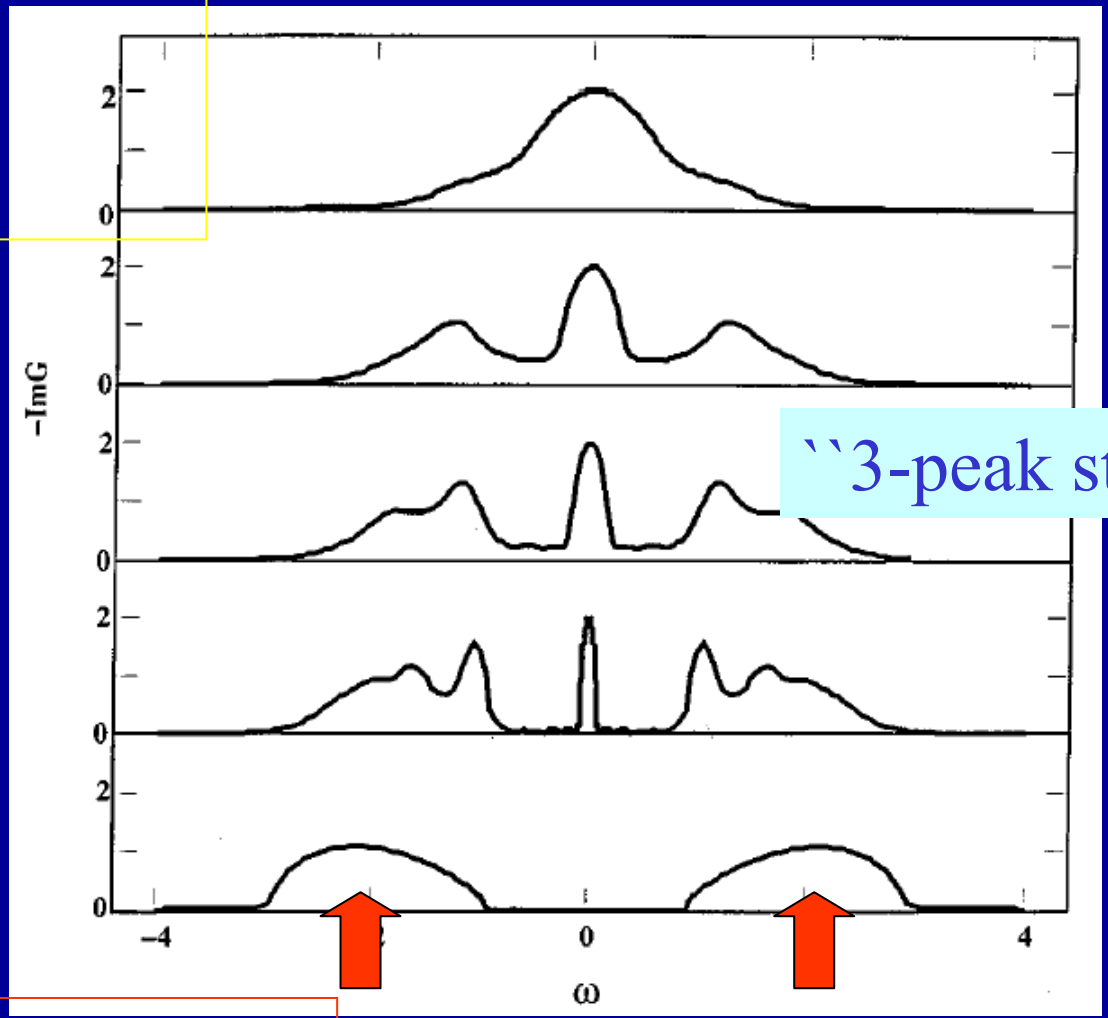

``3-peak structure''

Hubbard bands

> GAP <

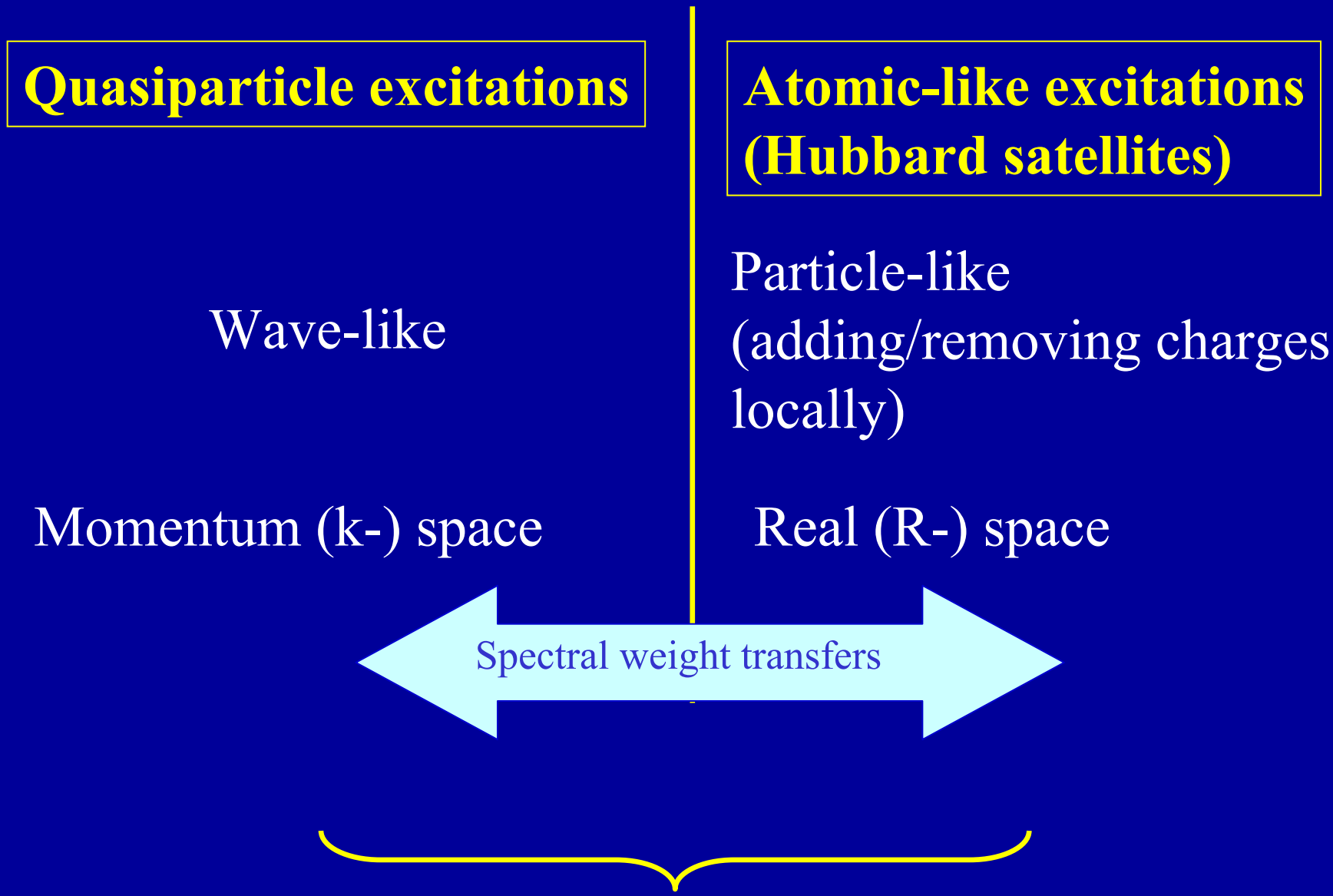
Quasiparticle excitations
Atomic-like excitations (Hubbard satellites)
Wave-like
Particle-like (adding/removing charges locally)
Momentum (k-) space
Real (R-) space
Spectral weight transfers
Are treated on equal footing within DMFT

VOLUME 69, NUMBER 12 PHYSICAL REVIEW LETTERS 21 SEPTEMBER 1992

Evolution of the Spectral Function in Mott-Hubbard Systems with d^1 Configuration

A.Fujimori et al.

Low-energy quasiparticles
and
high-energy Hubbard bands
coexist
in a strongly-correlated metal:
early evidence from photoemission (1992).
Independent theoretical evidence from DMFT (1991)

Tremendous experimental progress over the last ~ 12 years !

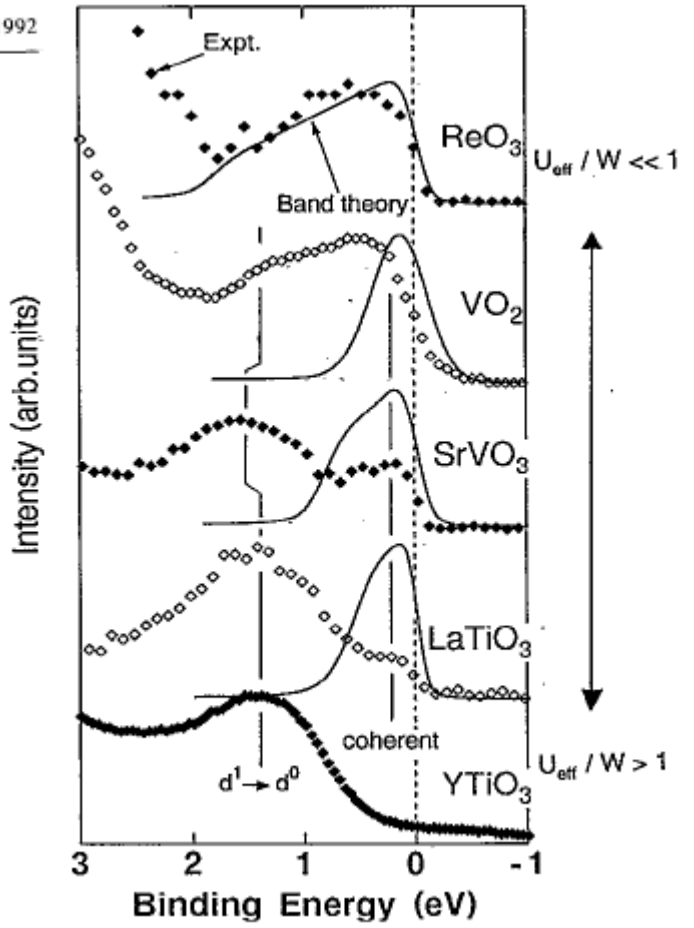

FIG. 2. Photoemission spectra (diamond symbols) of $YTiO_3$ ($h\nu$=21.2 eV), $LaTiO_3$ ($h\nu$=48 eV), and $SrVO_3$ ($h\nu$=55 eV) in the d-band region. The spectra of VO_2 in the metallic phase ($h\nu$=60 eV) and ReO_3 ($h\nu$=40.8 eV) are taken from Refs. [9] and [14], respectively. They are compared with the DOS given by band-structure calculations [13,15] (solid curves). The instrumental resolution is ~0.5 eV for VO_2 and ~0.2–0.3 eV otherwise.

PHOTOEMISSION…
A 12 years (success) story

Fujimori et al, 1992

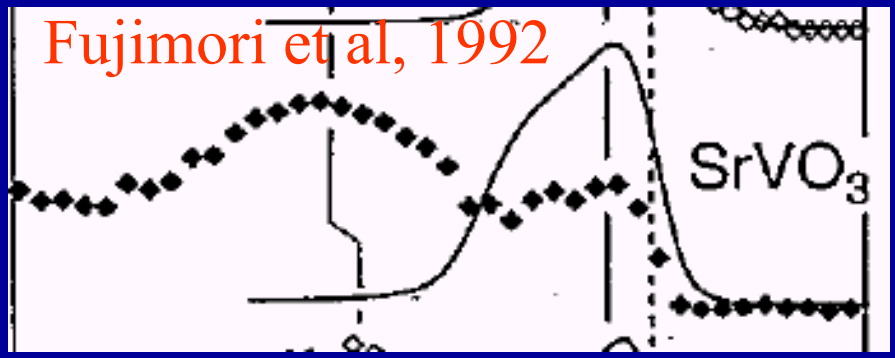

Maiti, Sarma et al., 1999

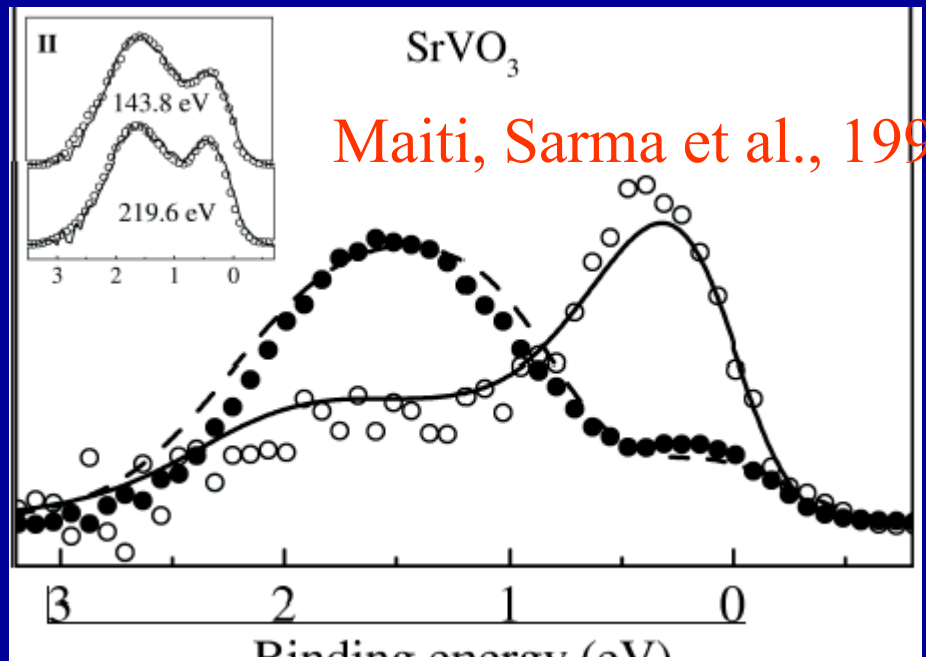

Inoue et al., 1995

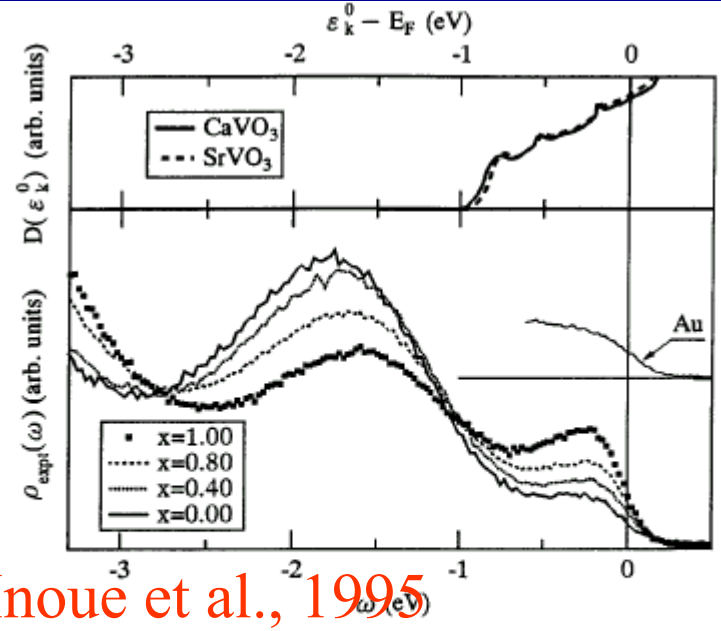

FIG. 1. Top: DOS $D(\varepsilon_k^0)$ of $CaVO_3$ and $SrVO_3$ calculated by the APW method. Bottom: measured photoemission spectra $\rho_{expt}(\omega)$ of $Ca_{1-x}Sr_xVO_3$ taken with $h\nu = 50$ eV. A spectrum of Au is also shown as a reference to E_F and the instrumental resolution.

Sekiyama et al., 2001

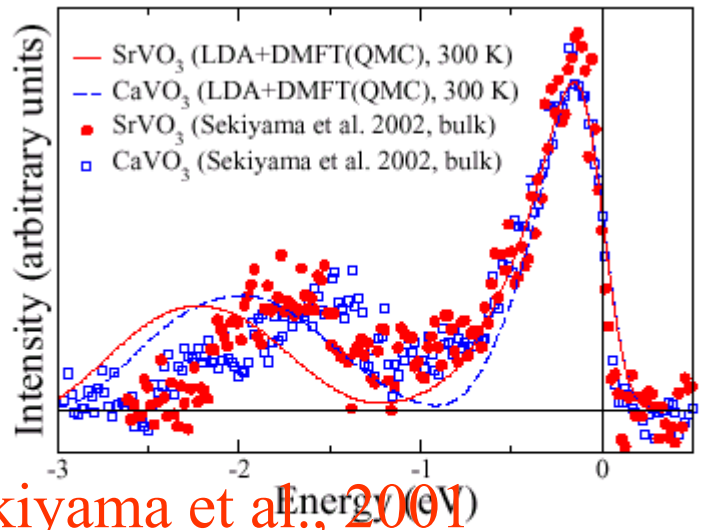

FIG. 4: Comparison of the calculated, parameter-free LDA+DMFT(QMC) spectra of $SrVO_3$ (solid line) and $CaVO_3$ (dashed line) with bulk-sensitive high-resolution PES ($SrVO_3$: circles; $CaVO_3$: rectangles) [4]. Horizontal line: experimental subtraction of the background intensity.

Quasiparticle peak revaled in recent **high-energy** photoemission experiments !

VOLUME 90, NUMBER 18 PHYSICAL REVIEW LETTERS week ending 9 MAY 2003

Prominent Quasiparticle Peak in the Photoemission Spectrum of the Metallic Phase of V_2O_3

S.-K. Mo,[1] J. D. Denlinger,[2] H.-D. Kim,[3] J.-H. Park,[4] J.W. Allen,[1] A. Sekiyama,[5] A. Yamasaki,[5] K. Kadono,[5] S. Suga,[5] Y. Saitoh,[6] T. Muro,[7] P. Metcalf,[8] G. Keller,[9] K. Held,[10] V. Eyert,[11] V.I. Anisimov,[12] and D. Vollhardt[9]

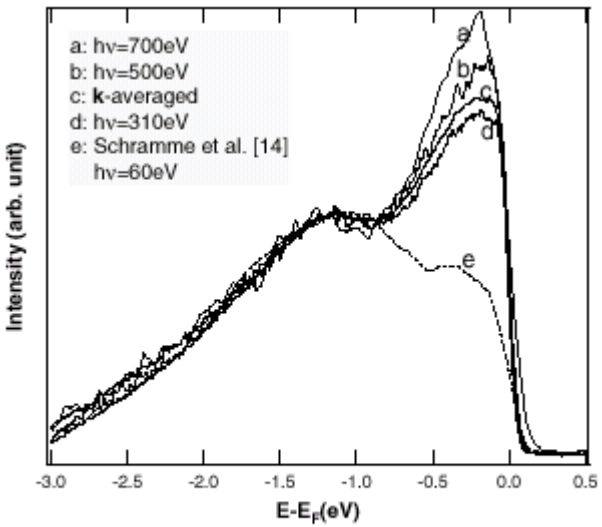

FIG. 2. PES spectra taken with various $h\nu$, the largest of which yields the greatest bulk sensitivity.

FIG. 3: (a) Bulk V 3d spectral functions of $SrVO_3$ (closed circles), $Sr_{0.5}Ca_{0.5}VO_3$ (solid line) and $CaVO_3$ (open squares). (b) Comparison of the experimentally obtained bulk V 3d spectral function of $SrVO_3$ (closed circles) to the V 3d partial density of states for $SrVO_3$ (dashed curve) obtained from the band-structure calculation, which has been broadened by the experimental resolution of 140 meV. The solid curve shows the same V 3d partial density of states but the energy is scaled down by a factor of 0.6.

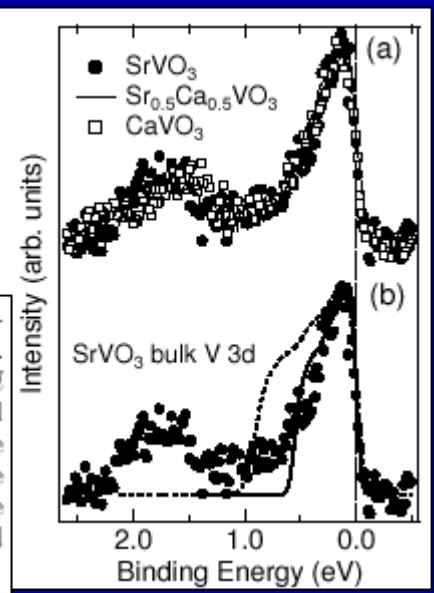

Genuine Electronic States Insensitive to the Distortion in Perovskite Vanadium Oxides Revealed by High-Energy Photoemission

A. Sekiyama,[1,*] H. Fujiwara,[1] S. Imada,[1] H. Eisaki,[2,†] S. I. Uchida,[2] K. Takegahara,[3] H. Harima,[4] Y. Saitoh,[5] and S. Suga[1]

Realistic DMFT Calculation of spectrum for an oxide: SrVO3

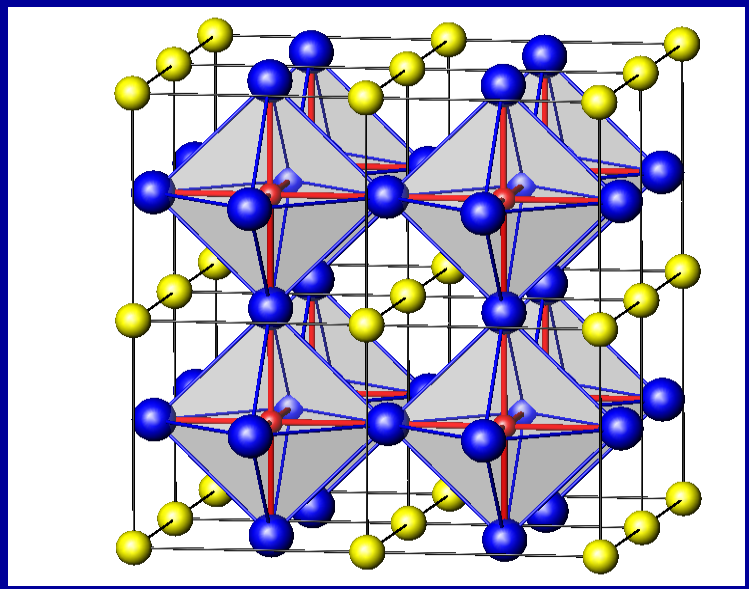

$SrVO_3$

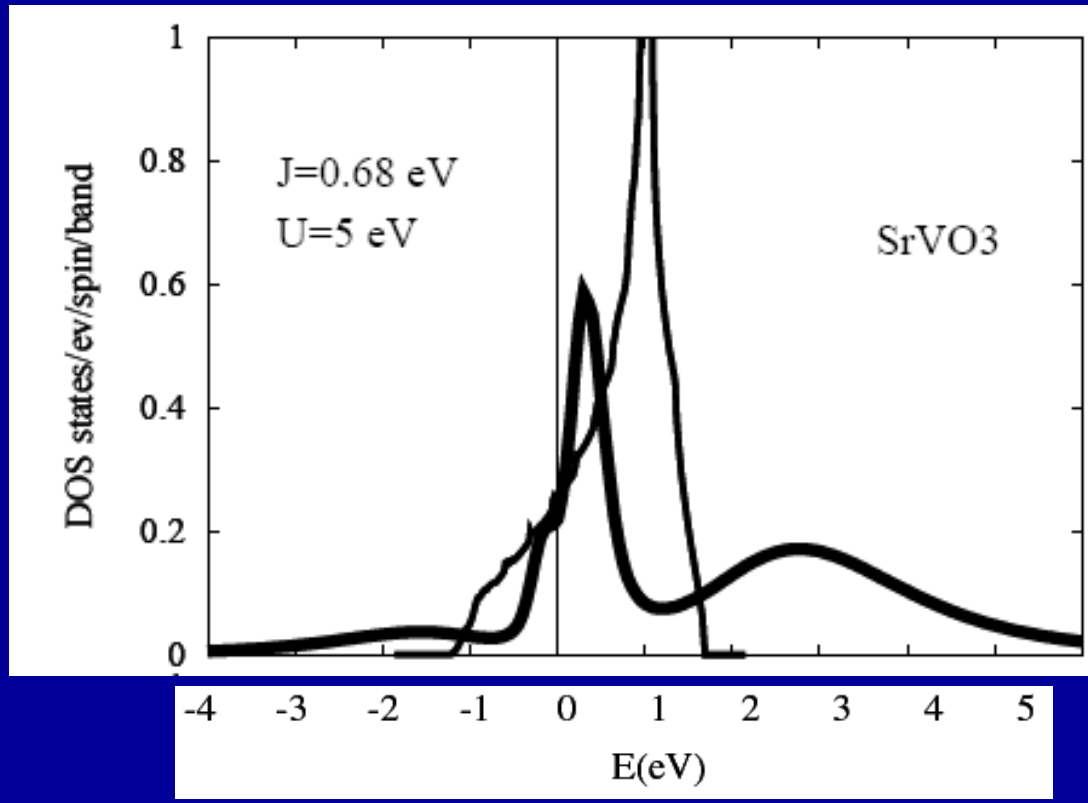

VOLUME 92, NUMBER 17 PHYSICAL REVIEW LETTERS week ending 30 APRIL 2004

Mott Transition and Suppression of Orbital Fluctuations in Orthorhombic $3d^1$ Perovskites

E. Pavarini,[1] S. Biermann,[2] A. Poteryaev,[3] A. I. Lichtenstein,[3] A. Georges,[2] and O. K. Andersen[4]

The strongly correlated metal at low-energy: ``single-parameter scaling''

(if only ω ~ ZD is considered → can be extended to a 2-parameter scaling up to scale ~ $Z^{1/2}$ D)

$$\mathrm{Im}\Sigma(\omega) = \mathrm{c}\,\mathrm{D}\phi\left(\frac{\omega}{\mathrm{ZD}}\right) \sim \mathrm{c}\frac{\omega^2}{\mathrm{Z^2D}} + \cdots$$

Consequences:

-Kadowaki-Woods ratio for resistivity vs. specific heat

-Behnia-Jaccard-Flouquet ratio for Seebeck vs. sp. heat

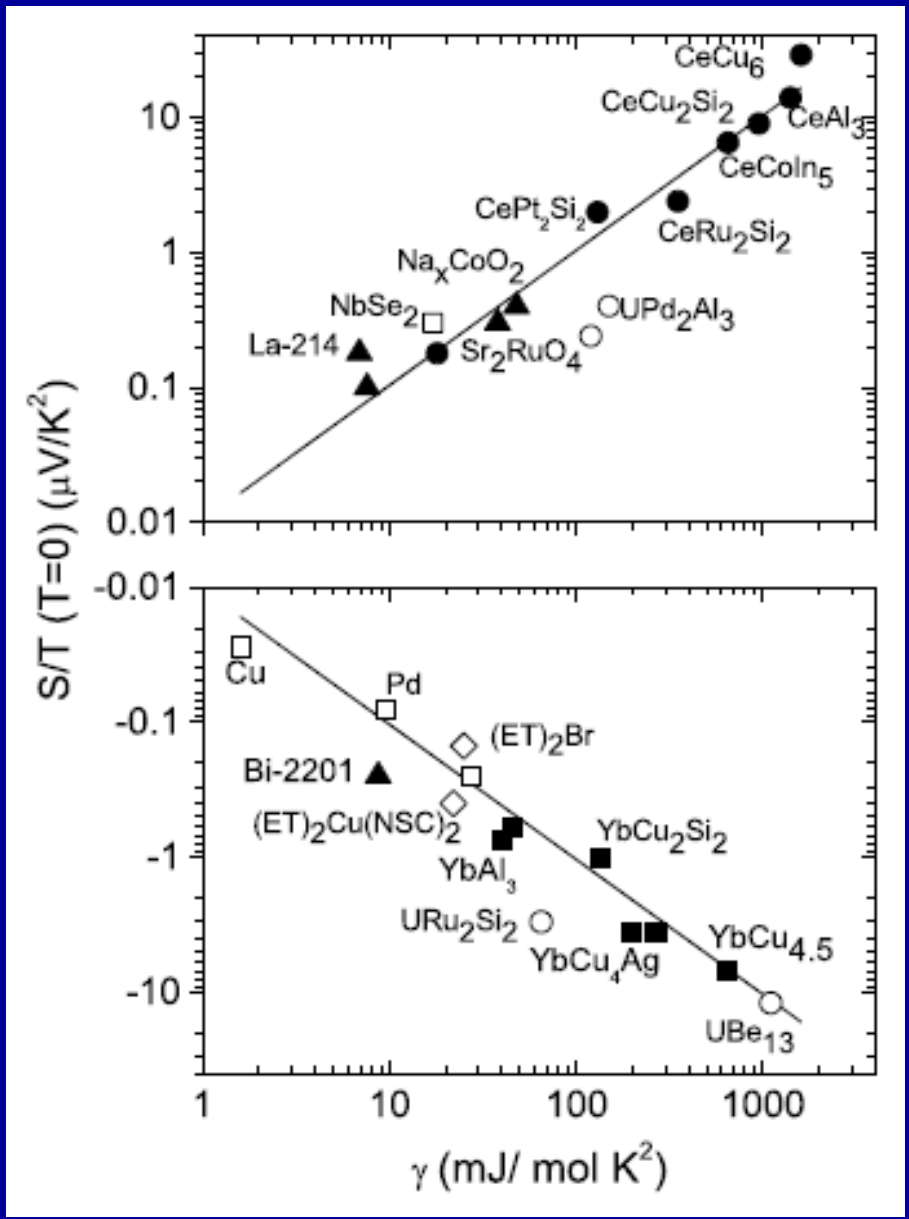

The Behnia-Jaccard-Flouquet ratio: S/Tγ

INSTITUTE OF PHYSICS PUBLISHING JOURNAL OF PHYSICS: CONDENSED MATTER
J. Phys.: Condens. Matter **16** (2004) 5187–5198 PII: S0953-8984(04)80129-2

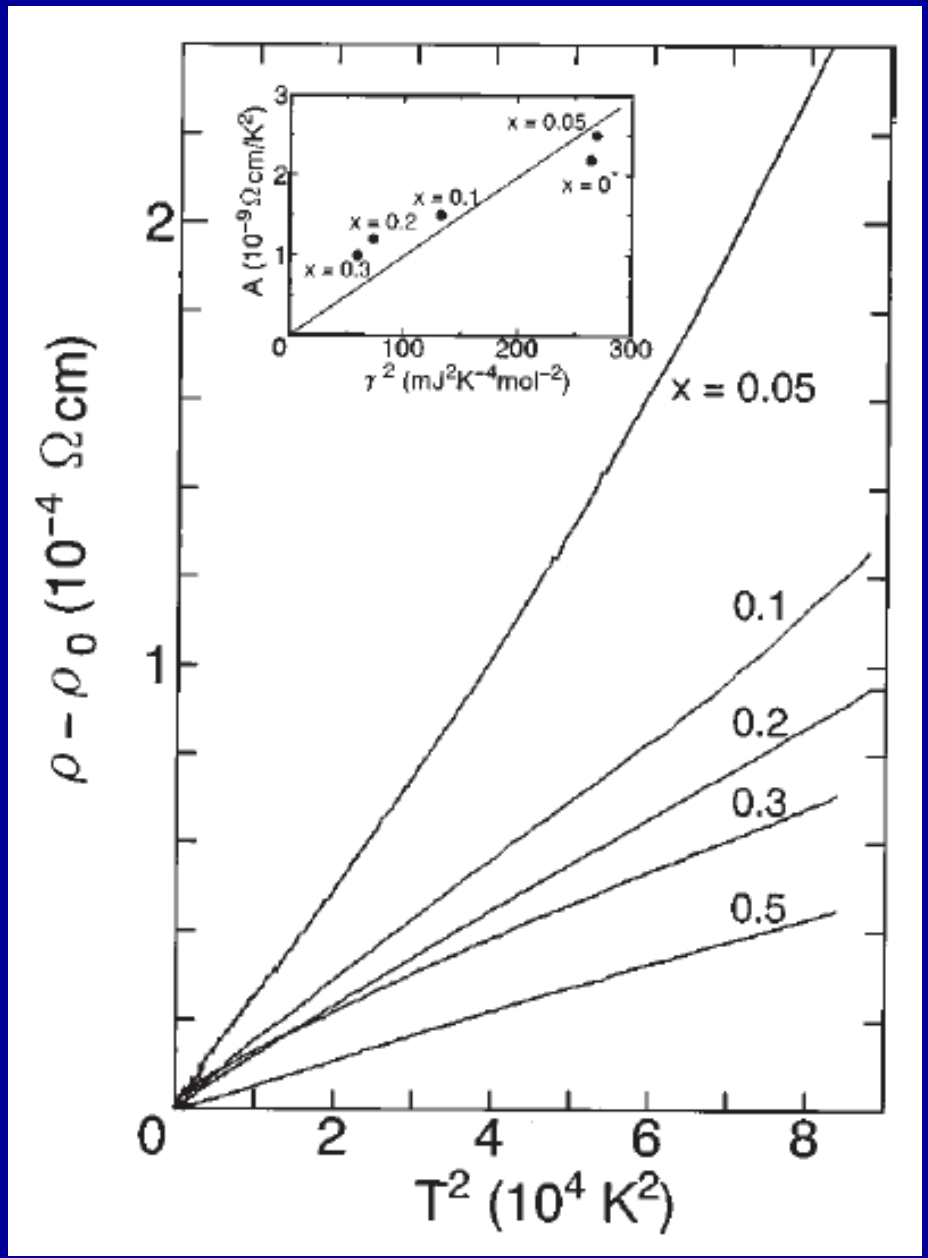

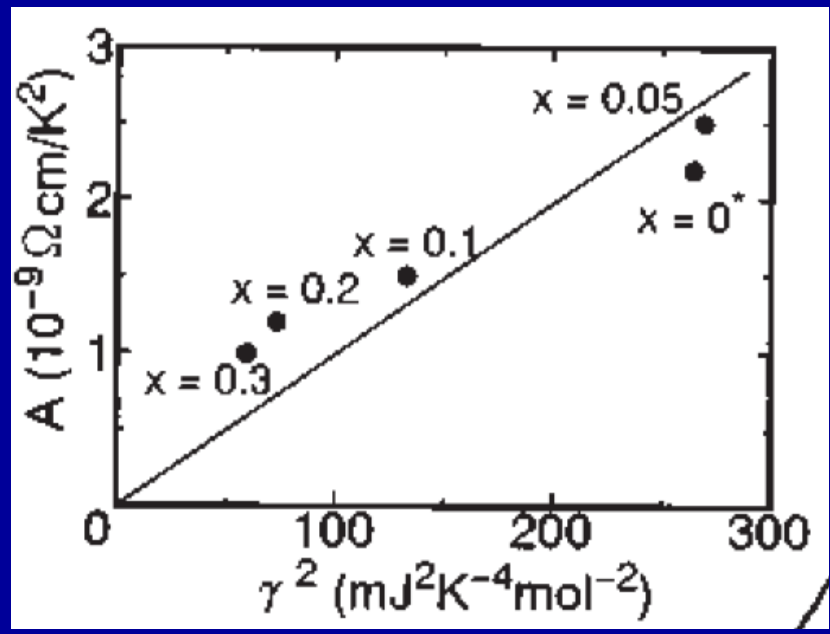

Titanates/transport:

$$\rho_{dc} = AT^2 + \cdots$$

$$A/\gamma^2 \sim \text{const.}$$

Fermi liquid behavior observed
Below ~ 100K @ 5% doping

Kadowaki-Woods ratio

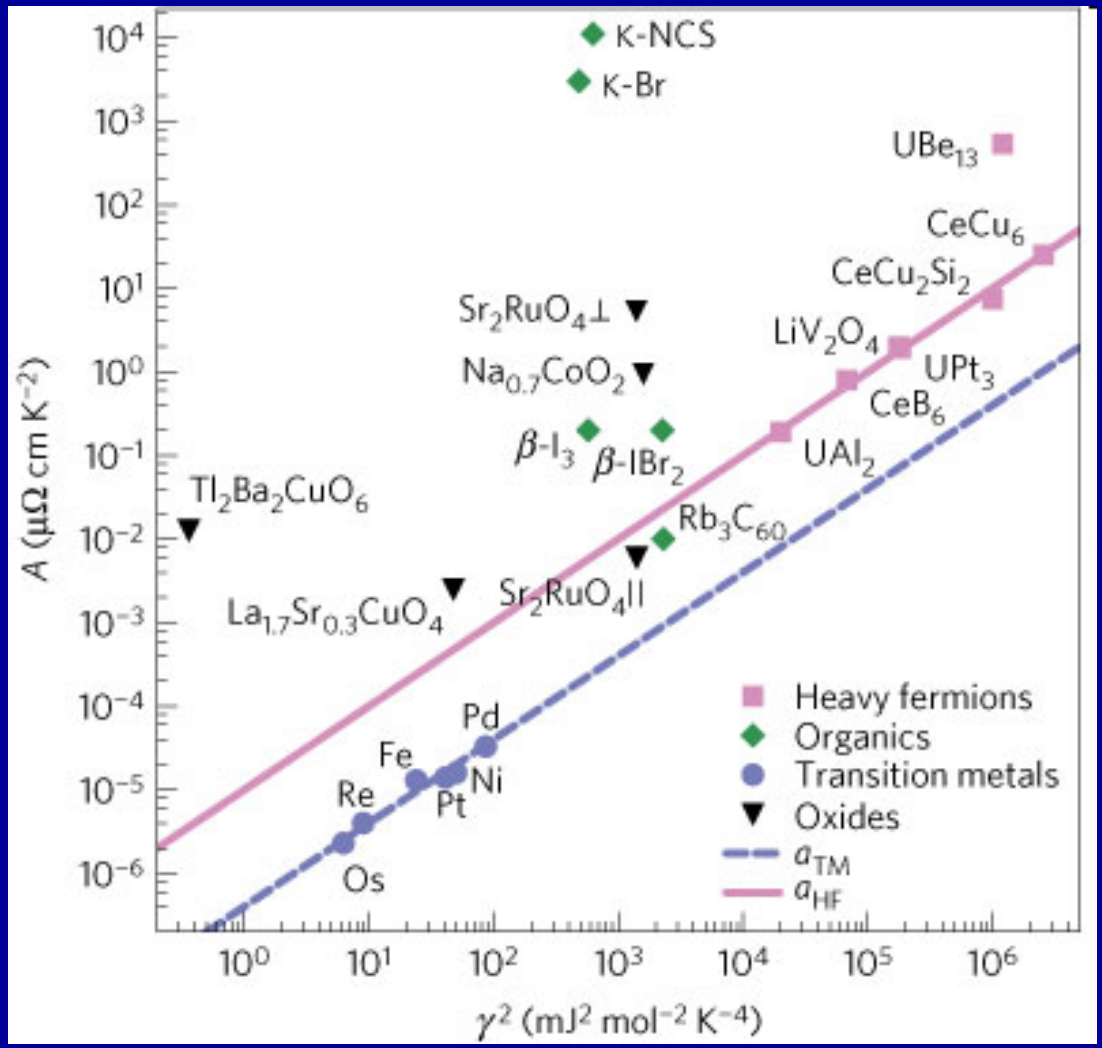

C- The paramagnetic Mott insulator DMFT viewpoint (i.e realistic for T not too low, weak magnetic correlations)

- Local moments
- Ln2 entropy per site
- Diverging local susceptibility
- Magnetic correlations show up in 2-particle quantities, not 1-particle (limitation of DMFT)
- Finite uniform q=0 susceptibiity ~ 1/J
- Pole in $\Sigma(\omega)$ related to gap

$$\mathrm{Im}\Sigma(\omega+i0^+) = -\pi\rho_2\delta(\omega) \quad \text{for} \quad \omega\in[-\Delta_g/2,\Delta_g/2]$$

$$\mathrm{Re}\Sigma(\omega+i0^+) - U/2 = \frac{\rho_2}{\omega} + O(\omega).$$

$$\frac{1}{\rho_2} = \int_{-\infty}^{+\infty} d\epsilon\, \frac{\rho(\epsilon)}{\epsilon^2}.$$

- Insulating solution : $\Delta(0) = 0$: gapped bath $\Rightarrow$ no Kondo effect

Spectral function (U/D=4)

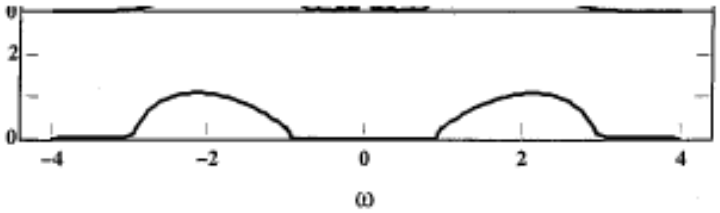

Self-energies in insulator

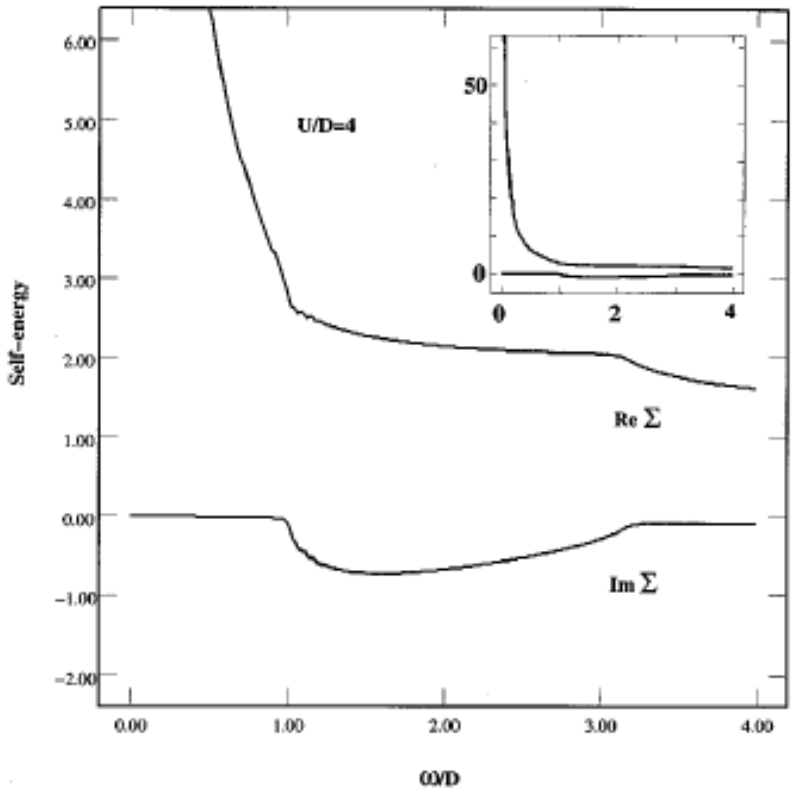

Atomic limit

$$G(i\omega_n) = \frac{1}{2}\left(\frac{1}{i\omega_n + U/2} + \frac{1}{i\omega_n - U/2}\right)$$

$$\Sigma(i\omega_n) = \frac{U^2}{2i\omega_n}$$

D- Thermodynamics :

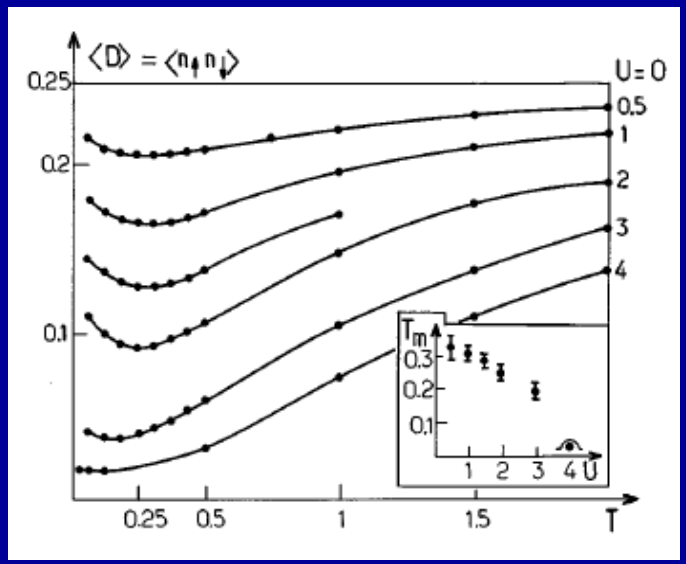

Pomeranchuk effect
In metal !

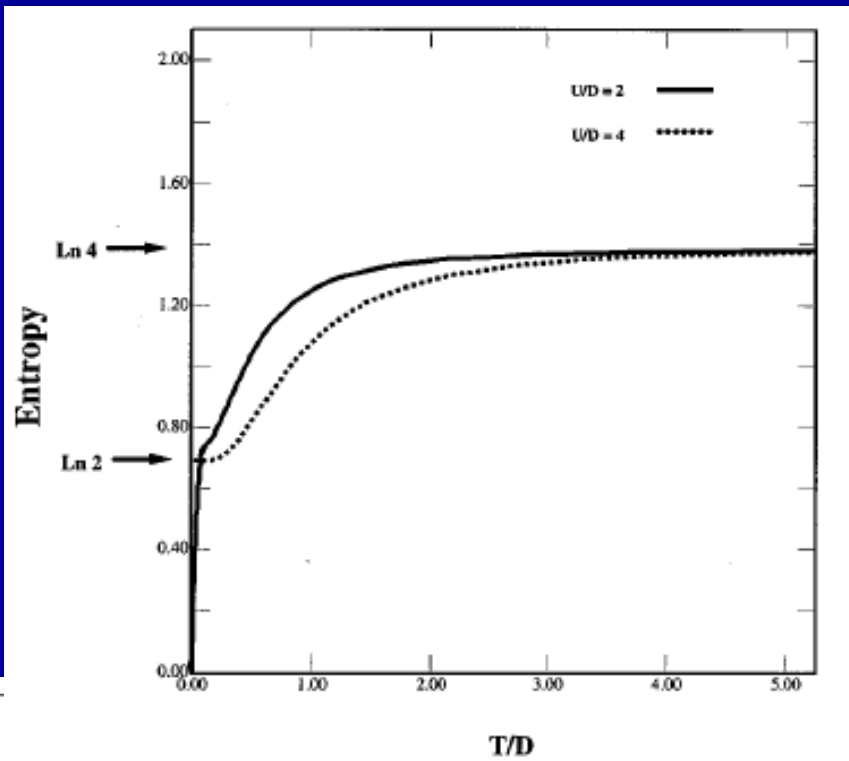

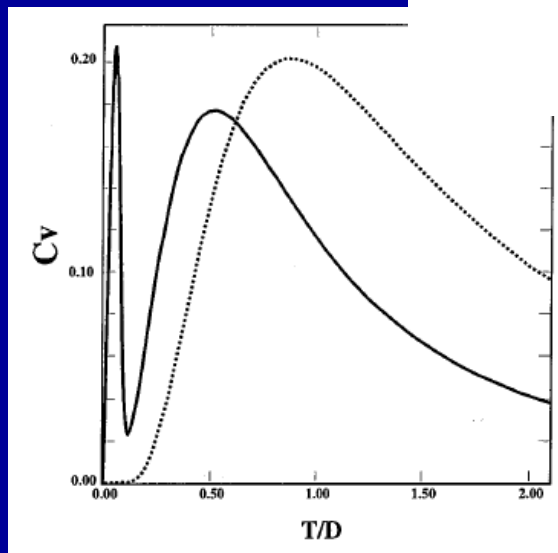

E- Fragile quasiparticles: materials with small quasiparticle coherence scale (e.g close to Mott transition):

- Large spectral weight transfers upon changing temperature
- Unconventional transport

QP coherence scale ~ width of quasiparticle band

$$\varepsilon_F^* \sim ZD$$

→ Because DMFT describes BOTH low-energy quasiparticles and incoherent Hubbard bands, these issues can be addressed and computed

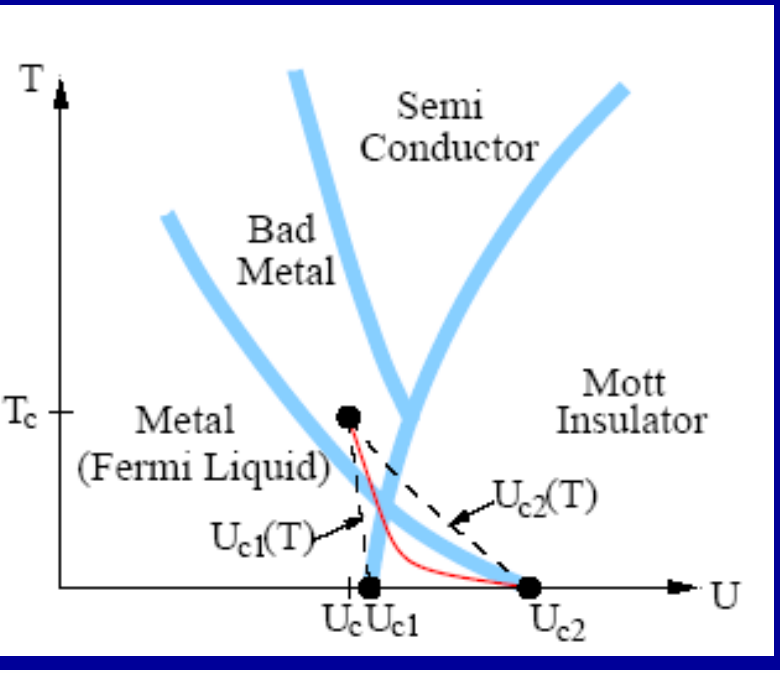

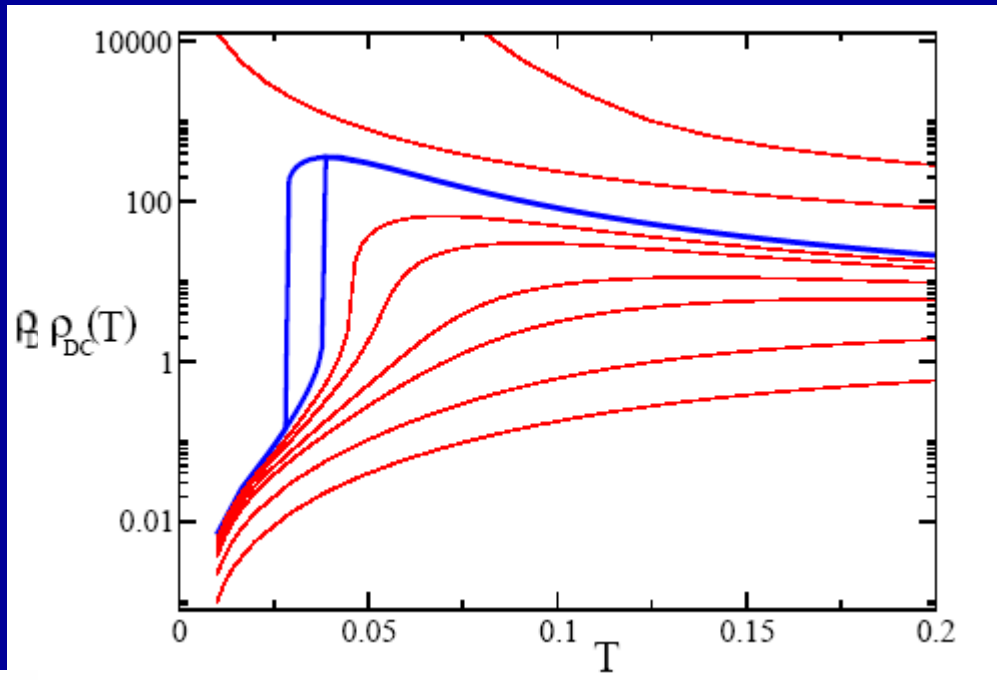

- *Fermi-liquid regime* $T \ll \epsilon_F^*$. Coherent quasiparticles. QP peak in the spectral function. Resistivity:

$$\rho = \rho_M \left(\frac{T}{\epsilon_F^*}\right)^2 \qquad (1)$$

Note: prefactor enhanced by correlations. $\rho_M \propto ha/e^2$ Mott value.

- *Incoherent ("bad") metal* $T \sim \epsilon_F^*$. QP peak quickly suppressed upon increasing T above ϵ_F^*. Resistivity is quasi-linear, and *greater than Mott limit.*

- *Insulating-like* $\epsilon_F^* \ll T \ll \Delta_g$. QP peak is gone. (Pseudo-) gap in local d.o.s. Transport is insulating-like (Mott gap).

Various regimes around the critical point

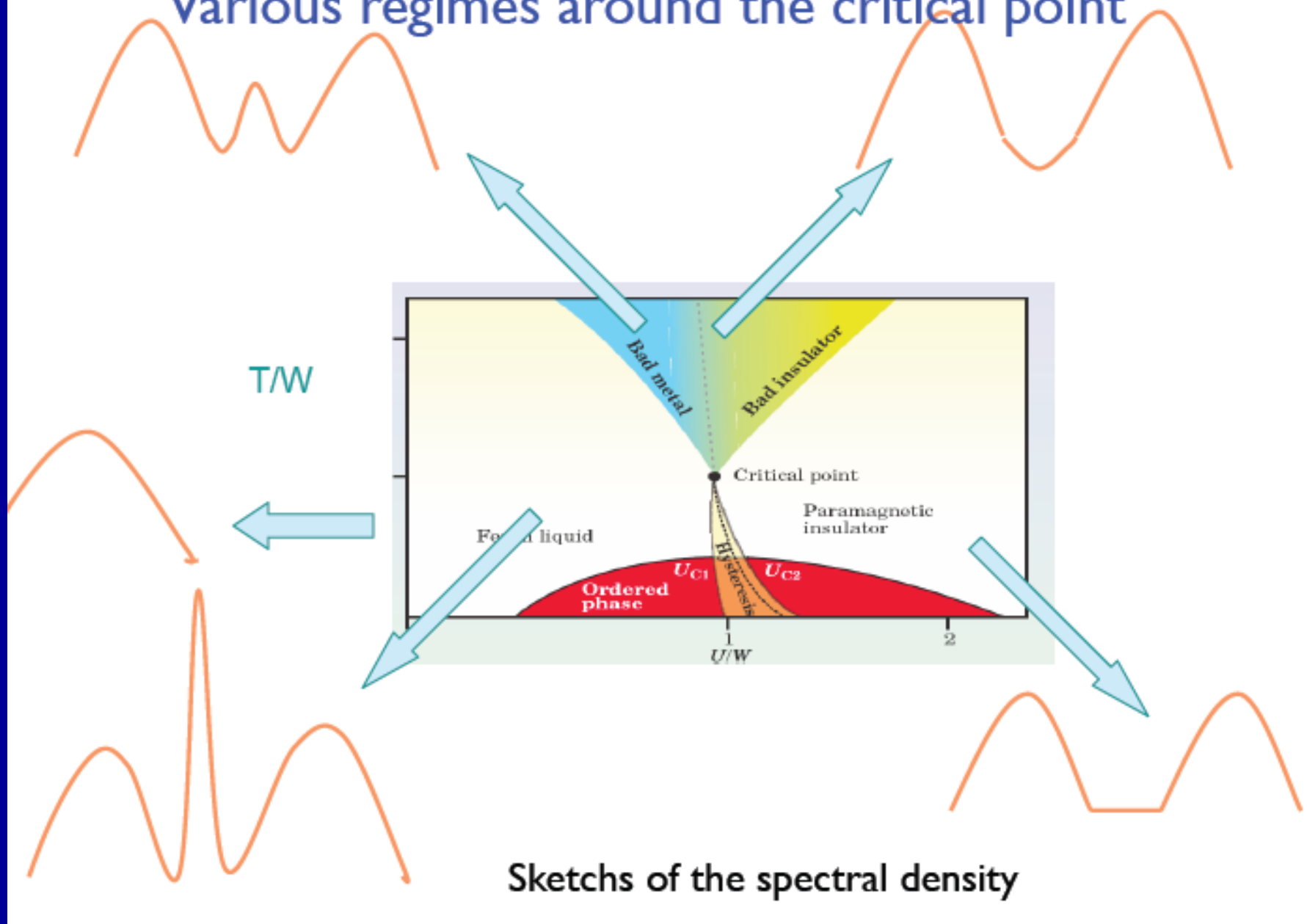

Sketchs of the spectral density

Mott transition and transport crossovers in the organic compound κ-(BEDT-TTF)$_2$Cu[N(CN)$_2$]Cl

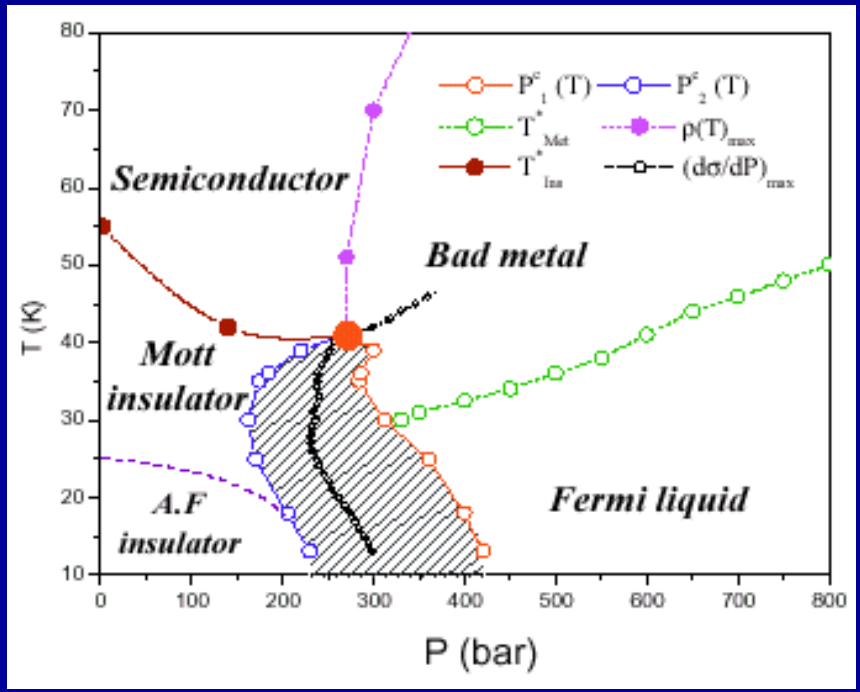

P. Limelette et al., PRL 91 (2003) 016401

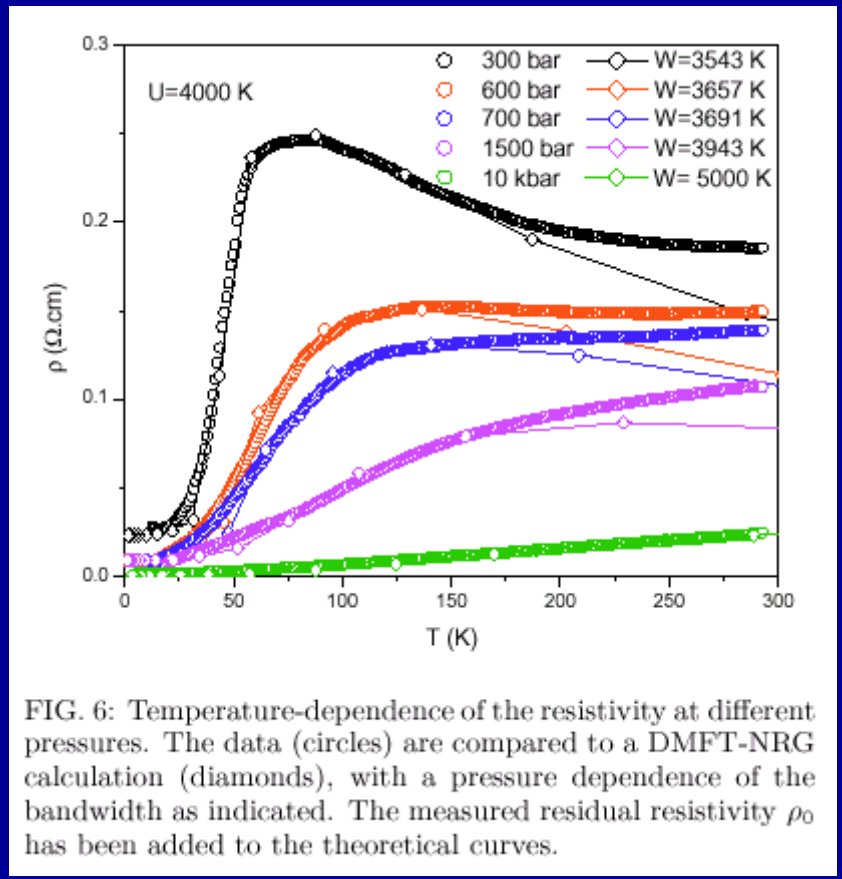

FIG. 6: Temperature-dependence of the resistivity at different pressures. The data (circles) are compared to a DMFT-NRG calculation (diamonds), with a pressure dependence of the bandwidth as indicated. The measured residual resistivity ρ_0 has been added to the theoretical curves.

DMFT/NRG calculations of resistivity (S.Florens.T.Costi.A.G)

Bad metal regime. Comparison with DMFT

- Bethe lattice, NRG solver
- Adjusted parameters :
  D, ρ(T=0), global scale and U.

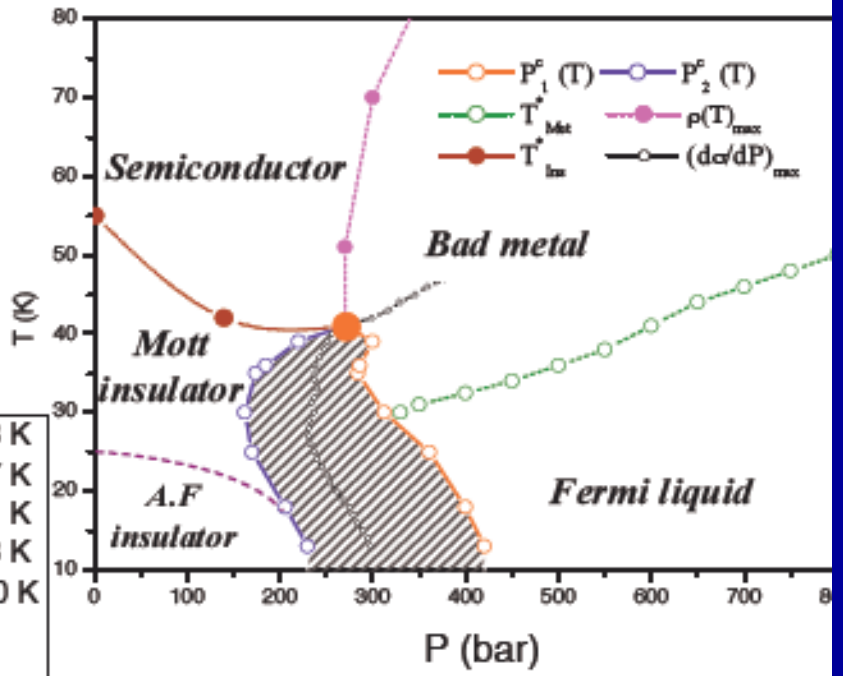

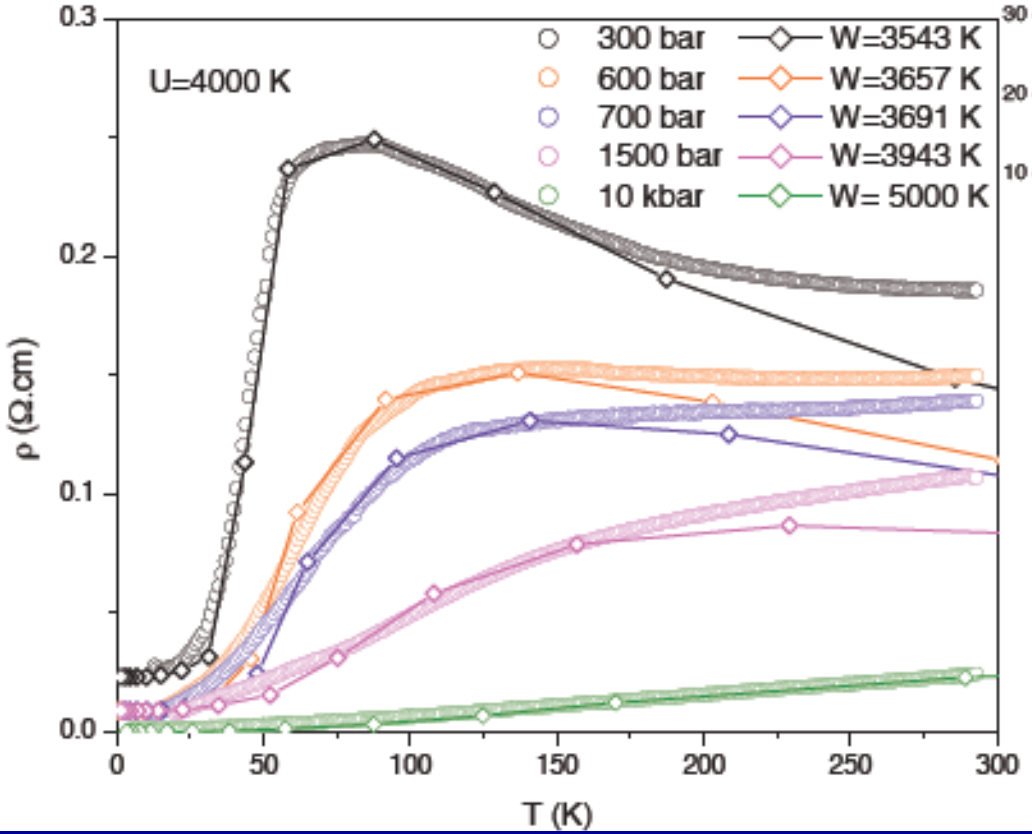

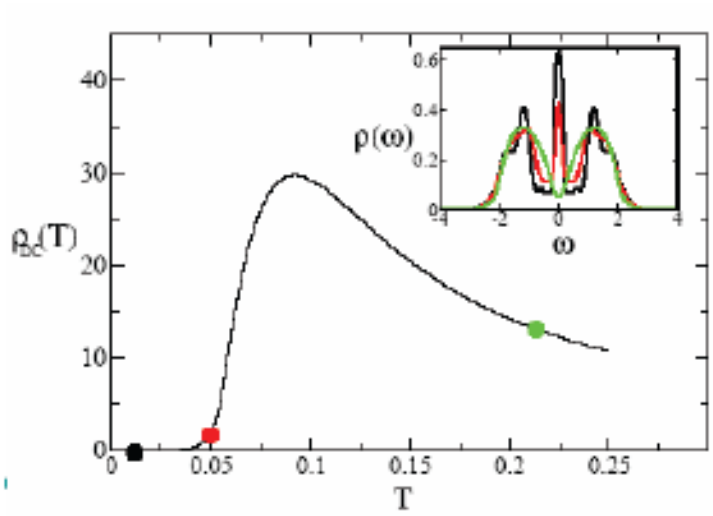

Large transfers of spectral weight seen in all spectroscopies, e.g optics:

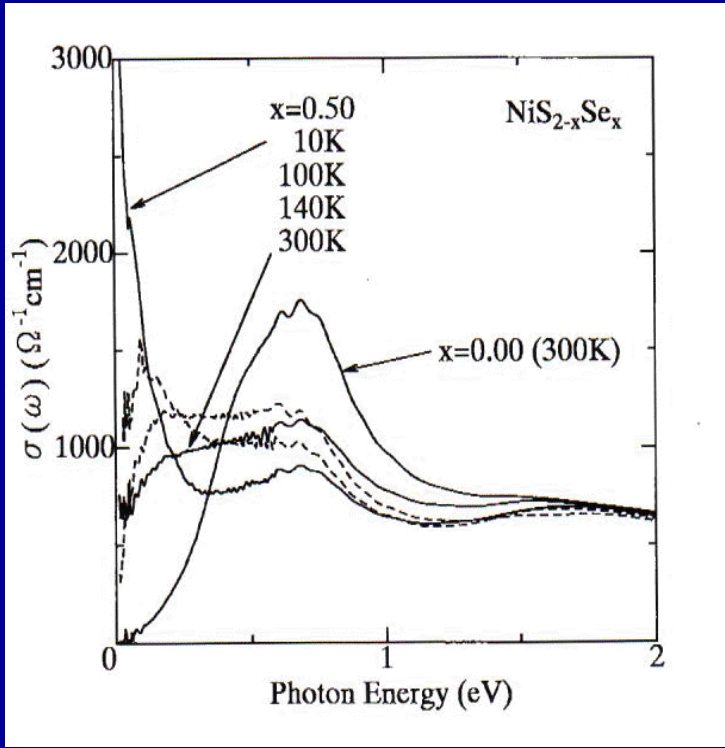

Miyasaka&Takagi, 2000

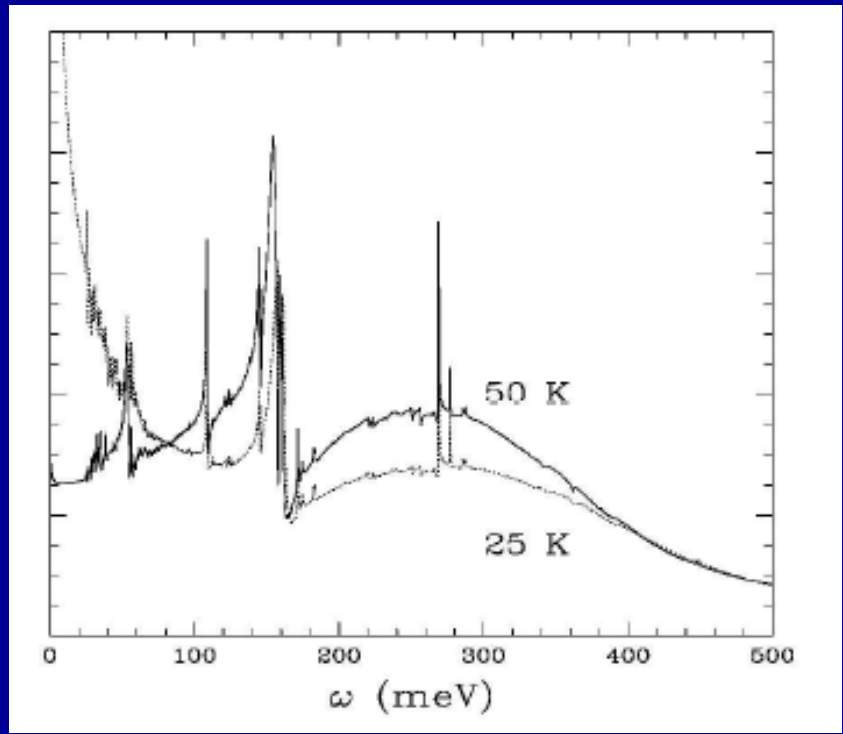

Optical conductivity of κ-(BEDT-TTF)$_2$Cu[N(CN)$_2$]Br at ambiant pressure [100], for $T = 25$K and $T = 50$K.

Optical conductivity

Drude weight ~ doping

FIG. 108. N_D to N_{D0} as a function of δ (Katsufuji, Okimoto, and Tokura, 1995) for $La_{1-x}Sr_xTiO_3$.

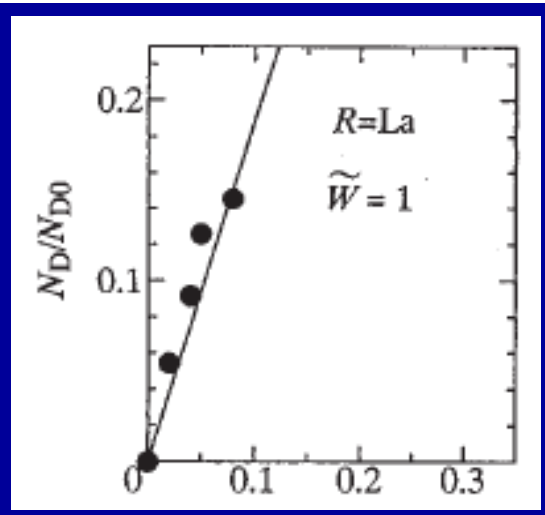

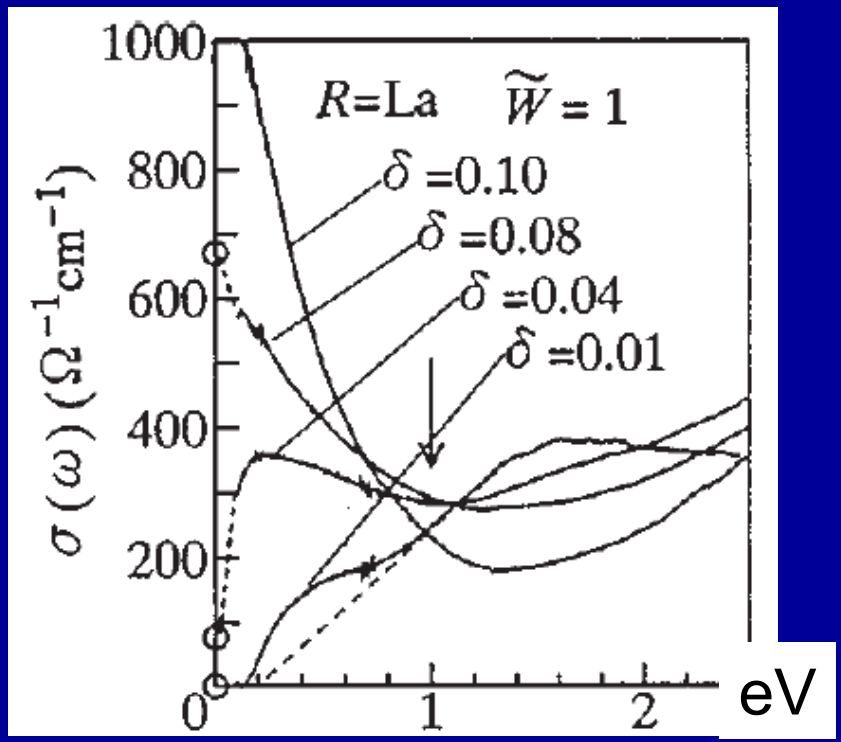

Large transfers of spectral weight

FIG. 107. Optical conductivity spectra in $R_{1-x}Sr_xTiO_{3+y}$ or $R_{1-x}Ca_xTiO_{3+y}$ (R=La, Nd, Sm, and Y). From Katsufuji, Okimoto, and Tokura, 1995.

Optics and transfers of spectral weight from DMFT calculations…

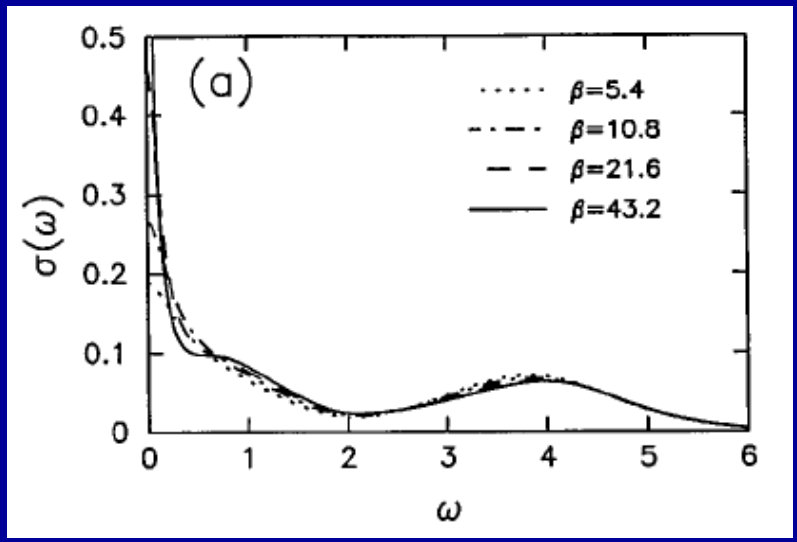

T-dependence

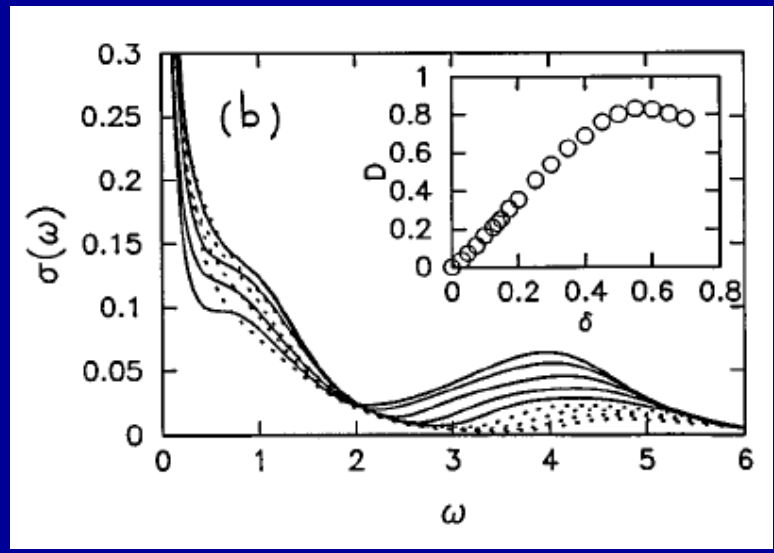

Doping-dependence

e.g. Rozenberg et al., 1995
Jarrell et al., 1995 (curves above)

Old results
→For much more recent work, see seminar by AJ Millis

Critical behaviour at the Mott critical endpoint

A liquid-gas transition ?

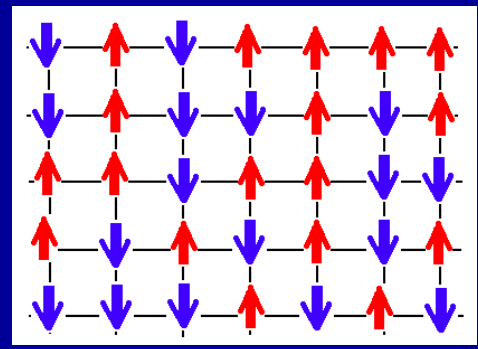

Insulator:

low-density of doubly occupied sites ➡ GAS

Metal:

High-density ➡ LIQUID

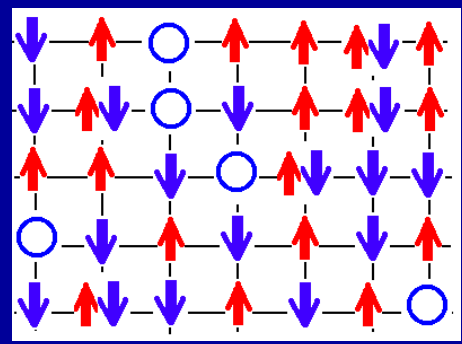

+ cf. early ideas of Castellani et al.

+ Recent DMFT/Landau theory approach: **scalar** order parameter

Critical behaviour near Tc,Uc

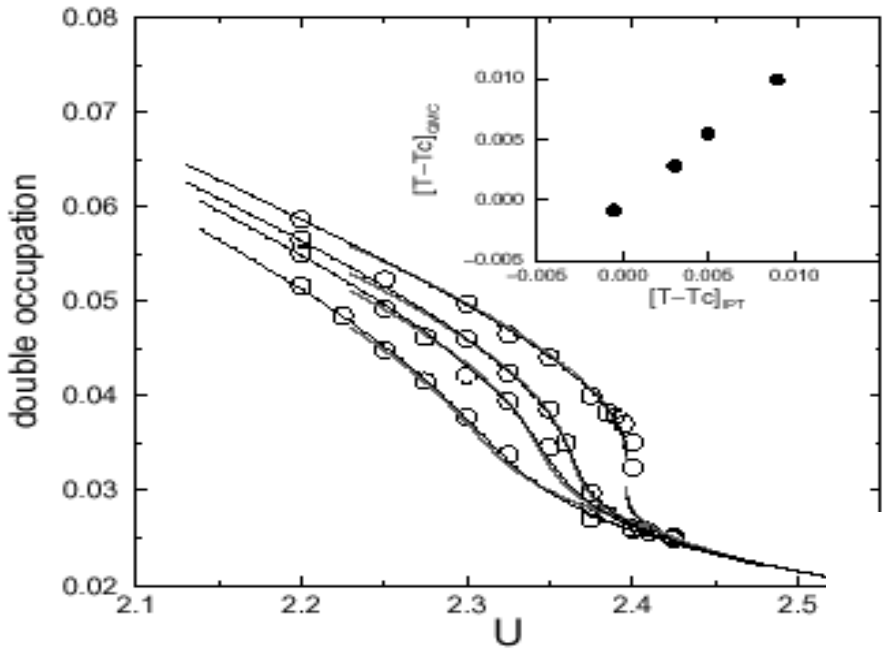

FIG. 1. Double occupation $\langle d \rangle$ as a function of U for dif
temperatures. The thin lines denote IPT results for T
0.0469, 0.05, 0.052, 0.056 (top to bottom). The thick lin
a fit to the IPT data using the LG theory. The circles are
data obtained at $T_{QMC} = 1/40, 1/35, 1/32, 1/25$ [8]. Th
results where shifted by a constant -0.07 along the U axi
by -0.003 along the $\langle d \rangle$ axis. The curves for the three
temperatures are above T_c and the lowest temperature one
branches) are just below. The inset shows the scaling
reduced temperatures $[T - T_c]_{QMC}$ versus $[T - T_c]_{IPT}$.

Kotliar et al. PRL 84 5180 (2000)

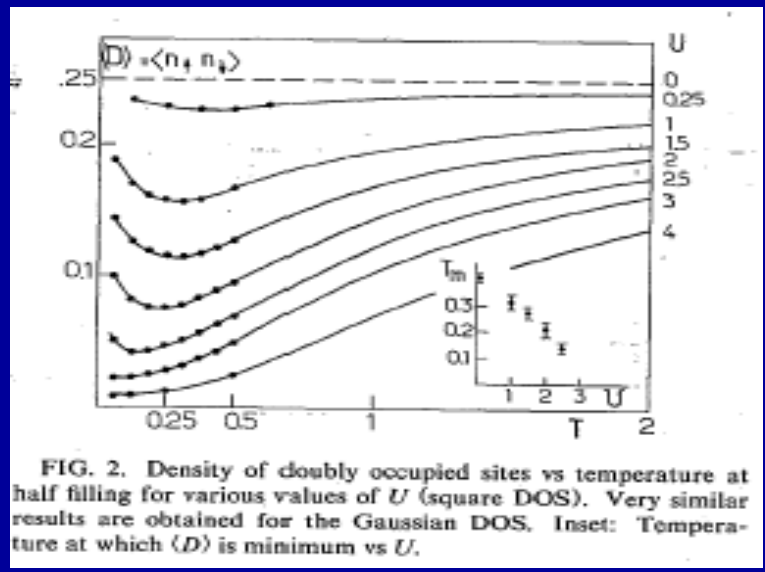

FIG. 2. Density of doubly occupied sites vs temperature at half filling for various values of U (square DOS). Very similar results are obtained for the Gaussian DOS. Inset: Temperature at which $\langle D \rangle$ is minimum vs U.

Georges and Krauth PRL 69 1240 (1992)

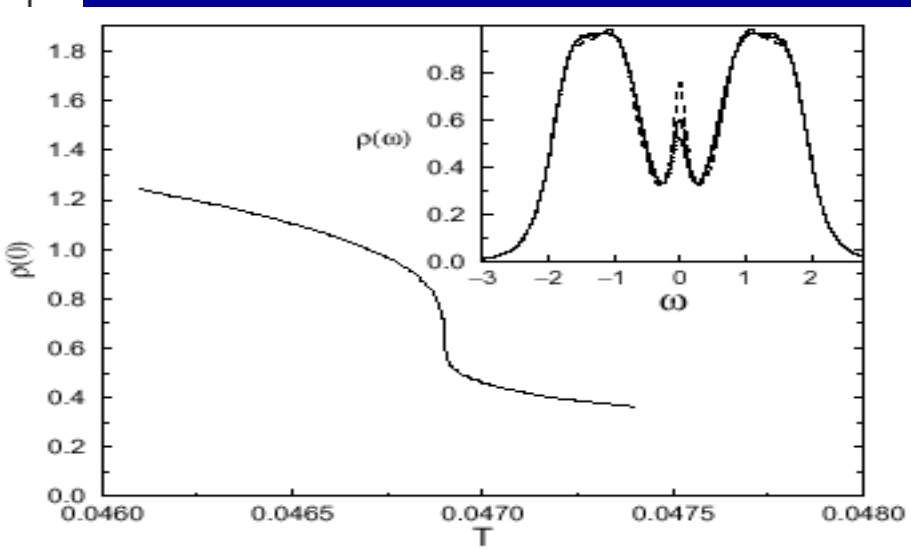

FIG. 2. The density of states at the Fermi energy $\rho(0) = A_0$ as a function of temperature in the critical region ($U = 2.463\,16 \approx U_c$). The singular behavior of the slope at $T_c \approx 0.046\,897$ can be clearly appreciated. The inset shows the variation of the spectral function for $U \approx U_c$ in the vicinity of T_c: dashed line for $T - T_c/T_c = -0.000\,25$, solid line for $T - T_c/T_c = 0.000\,06$, and dotted line for $T - T_c/T_c = 0.000\,49$ [11].

Cf.LIQUID-GAS transition

C. Liquid-gas critical endpoint

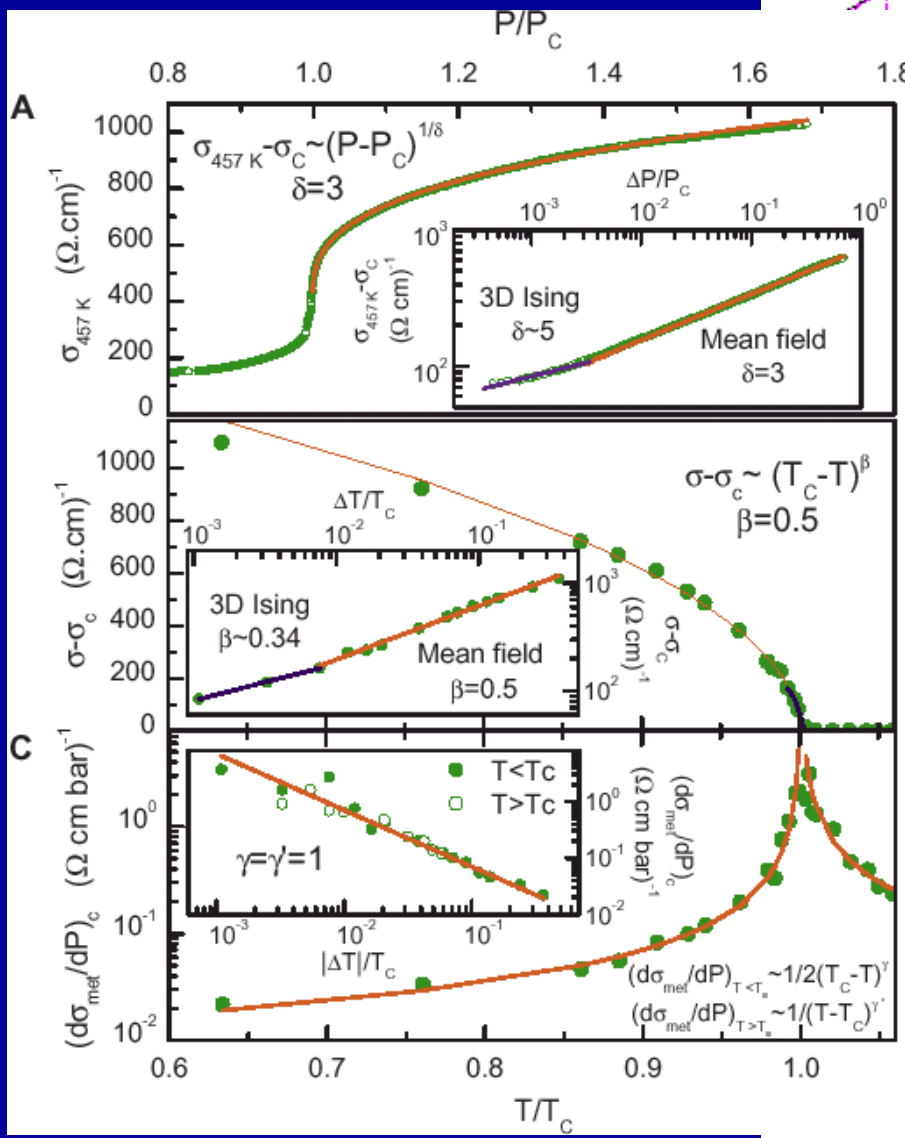

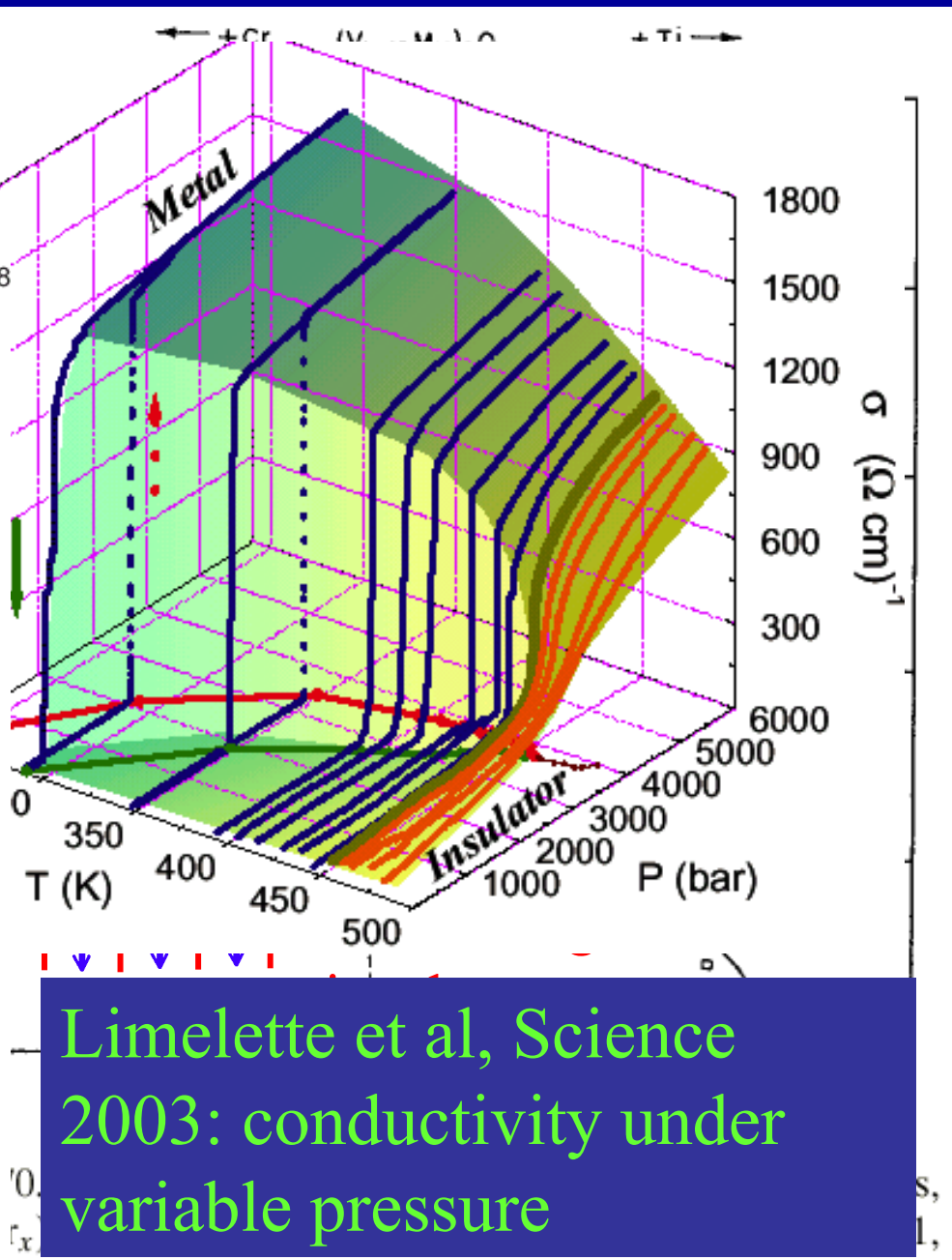

Limelette et al, Science 2003: conductivity under variable pressure

Scaling: Universal form of the ``equation of state''

$$\sigma_{met}(P,T) - \sigma_c = (\delta h)^{1/\delta} f_{\pm}\left(\frac{\delta h}{|r|^{\gamma\delta/(\delta-1)}}\right)$$

Cf also: Kagawa et al. (Kanoda's group) on the BEDT organics

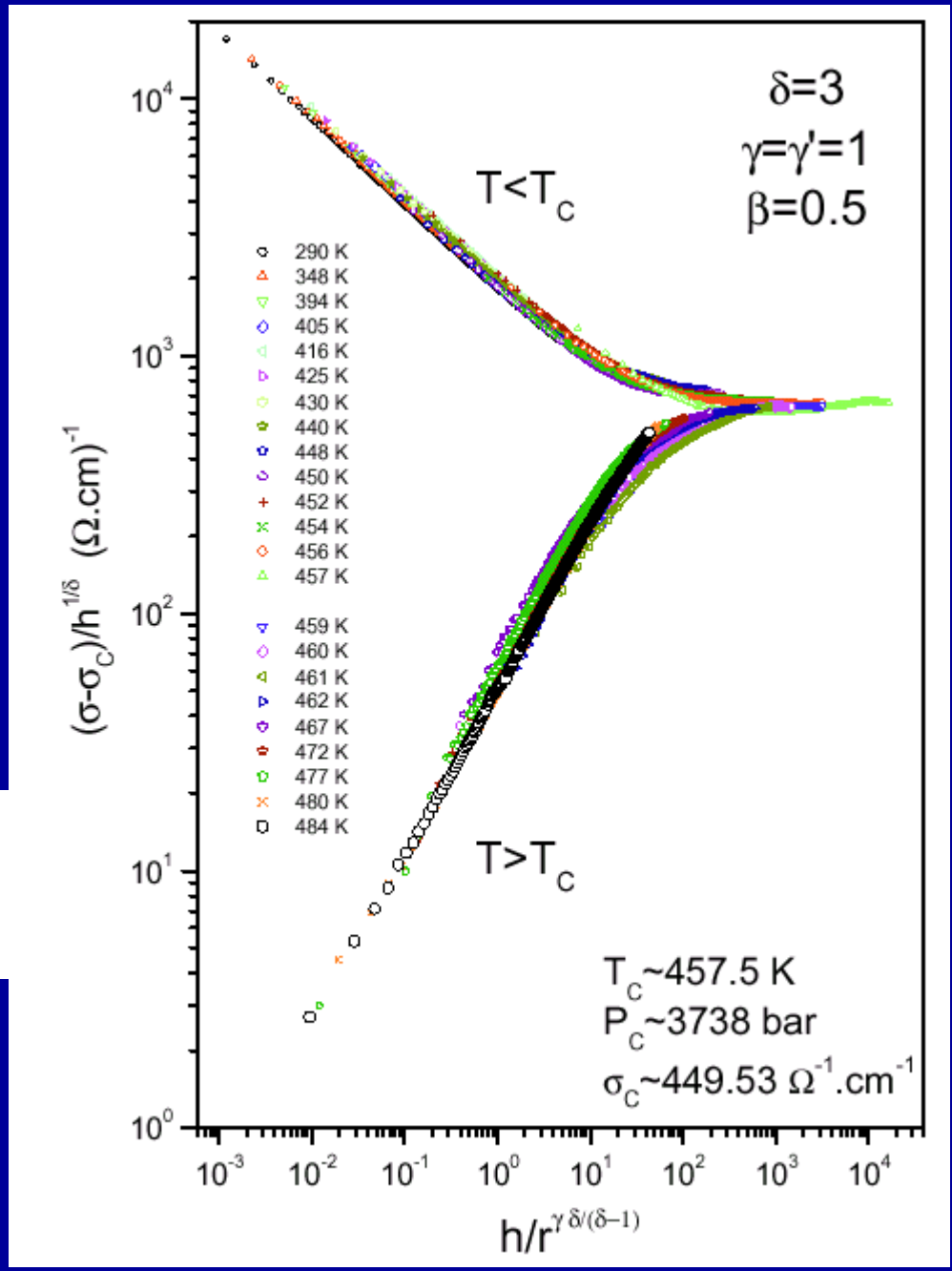

Beyond DMFT…

- Spatial correlations, when sizeable, influence quasiparticle properties

(e.g. cuts-off divergence of effective mass)

Some materials, especially hi-Tc cuprates at low doping levels, are strongly non-Brinkman Rice and follow a quite peculiar route to the Mott transition with strong momentum-space differentiation

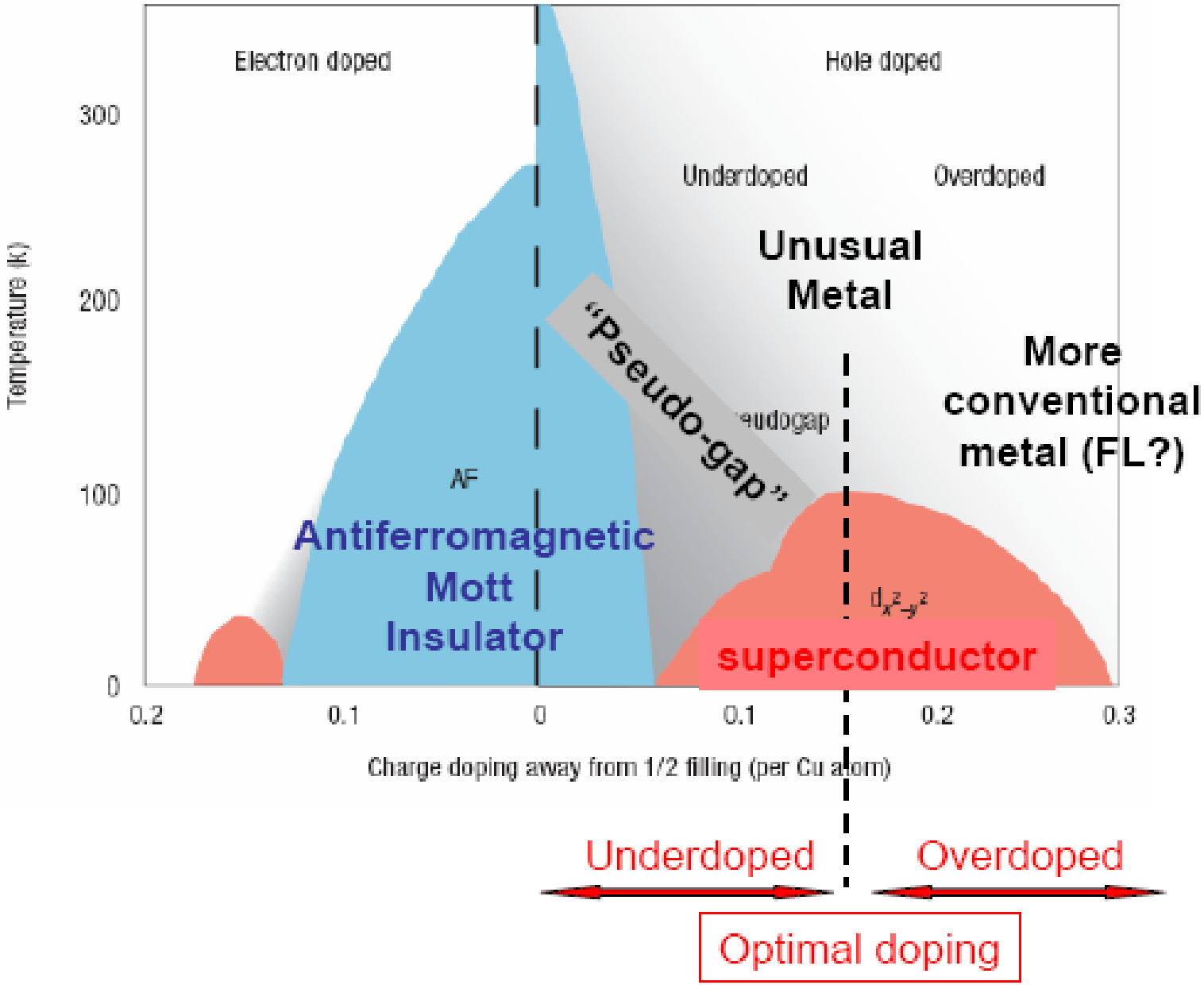
Electron doped
Hole doped
Underdoped
Overdoped
Unusual
Metal
"pseudo-gap"
More
conventional
metal (FL?)
AF
Antiferromagnetic
Mott
Insulator
superconductor
Temperature (K)
300
200
100
0
0.2
0.1
0
0.1
0.2
0.3
Charge doping away from 1/2 filling (per Cu atom)
Underdoped
Overdoped
Optimal doping

NORMAL state:

- ``Nodal'' regions display reasonably coherent quasiparticles
- In contrast, excitations in the ``antinodal'' regions e.g. (0,π) are much more incoherent

  AND they are (pseudo-) gapped below T*

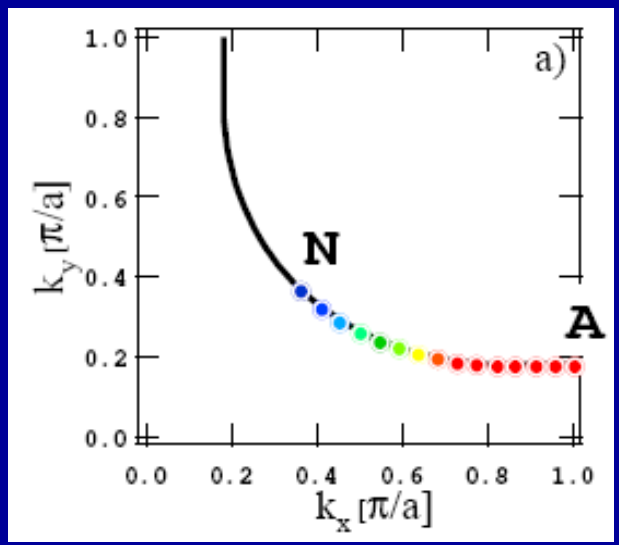

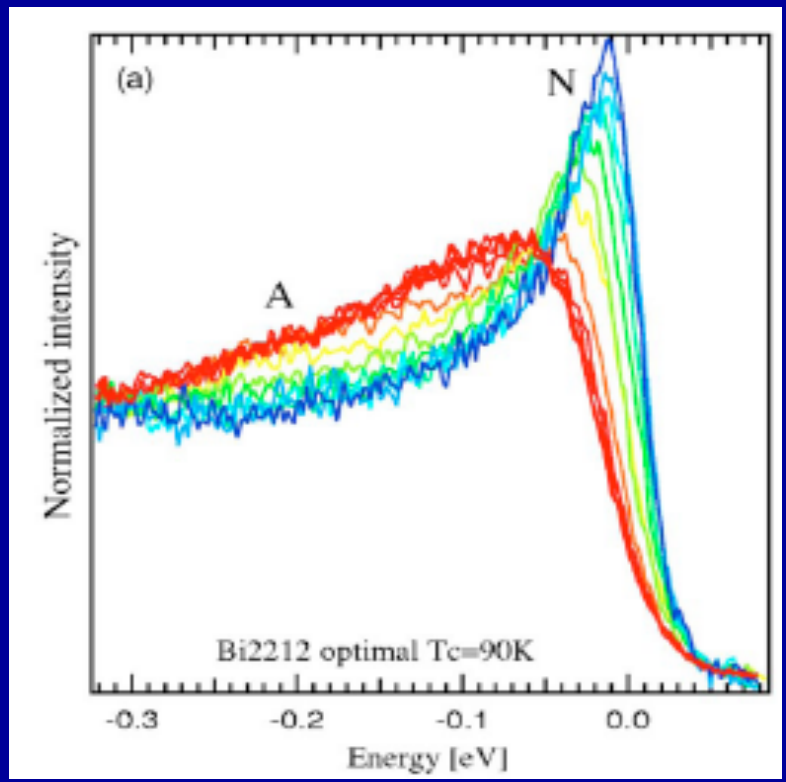

Kaminski et al., 2004 Bi2212
Tc=90K@T=140K

ARPES sees « Fermi arcs »

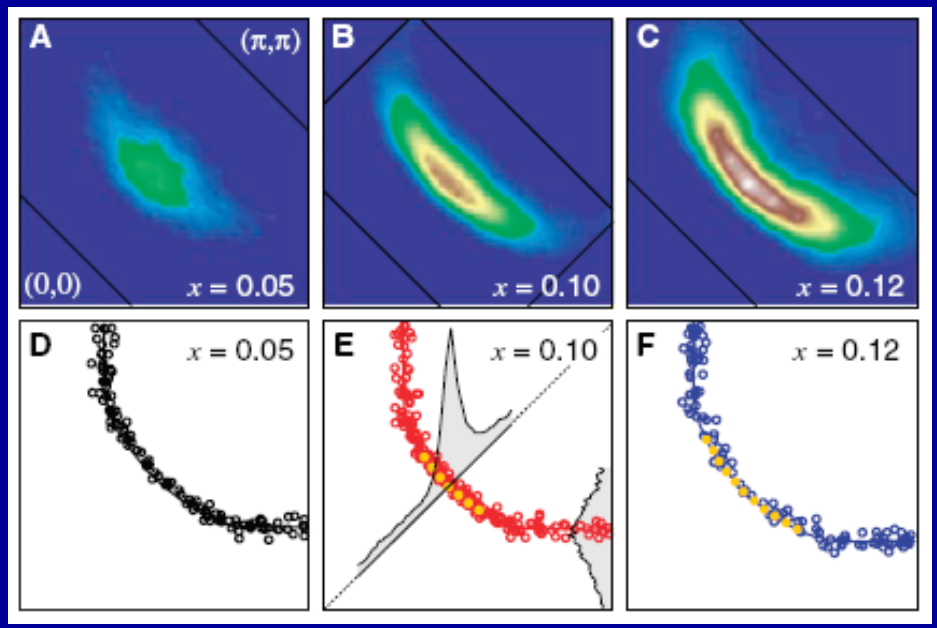

$Ca_{2-x}Na_xCuO_2Cl_2$

K.Shen et al. Science 2007

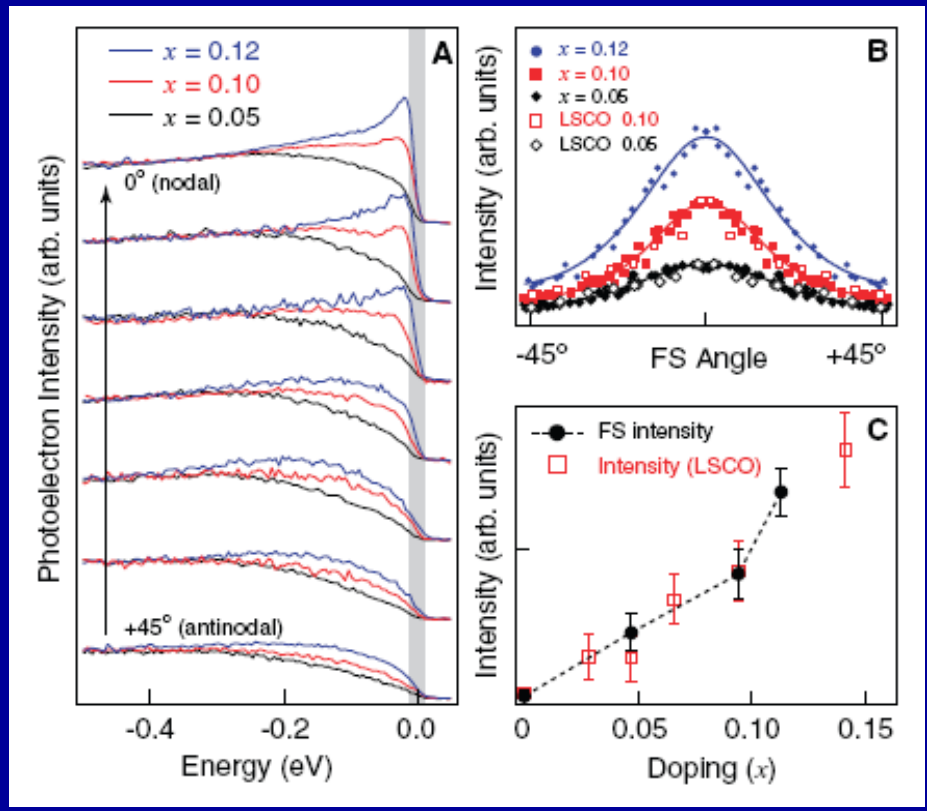

→Next year's lectures !
(Fall 2010)